Annu. Rev. Biophys. Biomol. Struct. 1992. 21:441–83

STRUCTURE AND MECHANISM OF ALKALINE PHOSPHATASE

Joseph E. Coleman

Department of Molecular Biophysics and Biochemistry, Yale University, New Haven, Connecticut 06510

KEY WORDS: zinc enzymes, enzyme mechanisms (alkaline phosphatase), crystal structure (alkaline phosphatase), ^{31}P NMR (alkaline phosphatase), ^{113}Cd NMR (alkaline phosphatase)

CONTENTS

1056–8700/92/0610–0441$02.00

INTRODUCTION

Alkaline phosphatase is often cited as the most frequently referenced enzyme (55). This fact relates more to the widespread use of alkaline phosphatase activity in human serum as an enzymatic signal for a variety of disease states involving particularly the liver and bone, than to a greater number of investigations directed at the molecular properties of the enzyme. The emergence in the literature of the enzyme alkaline phosphatase began around 1907 when Suzuki et al first suggested that phosphatases constituted a separate class of eukaryotic enzymes (70). By 1912, the enzyme we now know as alkaline phosphatase was defined by the work of Grosser & Husler (40) and von Euler (75), who showed that while it was present in a variety of tissues, the enzyme, which could hydrolyze glycerophosphate and fructose 1–6 diphosphate, was present in highest amount in intestinal mucosa. von Euler & Funke (76) used the word phosphatase for the first time in 1912. The enzyme from intestinal mucosa, particularly calf intestine, became the prototype for investigators exploring the properties of the enzyme itself.

Not until 1961 did Engstrom discover that the intestinal enzyme formed a phosphoseryl residue when incubated with phosphate esters at low pH (27, 28). The enzyme's catalysis of ^{18}O exchange into inorganic phosphate strongly supported the notion that the phosphoserine is a significant intermediate on the catalytic pathway (3, 65, 69). The demonstration that transfer of phosphate by the enzyme from an ester to a second alcohol leads to retention rather than inversion of configuration around the phosphorous (46) supported the conclusion derived from much previous evidence that the mechanism involves two sequential in-line nucleophilic attacks at phosphorous, the first by the hydroxyl of Ser102 on the incoming phosphomonoester and the second on the phosphoseryl intermediate by solvent water or an alcohol acceptor (32–34, 38).

In the late 1950s and early 1960s, investigators discovered that *Escherichia coli* possessed an alkaline phosphatase that was derepressible by phosphate starvation (21, 31, 42, 72). Its gene, *phoA*, was part of the *pho* regulon consisting of the group of genes in *E. coli* whose products are involved in phosphate transport and metabolism (4, 22, 38, 53) (for bibliography, see 22, 38). The *E. coli* enzyme had similar catalytic properties, similar pH-rate profile, and formed the same phosphoseryl intermediate as the intestinal enzyme (66, 67). The amino acid sequences of the mammalian enzymes, derived from their cDNA sequences, can be fit into the primary structure of the bacterial enzyme, with the proper adjustments for some insertions and deletions (47). With such adjustments, most of the critical active-site residues described below are conserved between the eukaryotic and bacterial enzymes.

In 1962, the *E. coli* alkaline phosphatase joined the class of zinc metalloenzymes with the demonstration by Plocke et al (62) that the enzyme contained stoichiometric amounts of zinc, a finding also confirmed in later studies of the calf intestinal enzyme (30). These early studies showed that Zn(II) is required for activity, and many subsequent studies have confirmed this observation, including the demonstration that the metal is required for initial phosphate binding and thus for the formation of the phosphoseryl intermediate (3). The great stability over a wide range of pH of the metal-free apophosphoryl enzyme, which can be formed by removal of the metal ion from the Cd(II) enzyme, demonstrates that the metal ion is required for dephosphorylation of the phosphoseryl intermediate as well (18).

The most detailed information on the structure and function of the enzyme is available for the *E. coli* enzyme. This review is a synthesis of the solution data and the recently completed crystal structures of the *E. coli* alkaline phosphatase and its two phosphoenzyme intermediates at 2.0-Å and 2.5-Å resolution, respectively (48). The phosphoenzymes are E·P, the noncovalent complex formed between inorganic phosphate and the enzyme, and E-P, the covalent or phosphoseryl intermediate, formed by the phosphorylation of Ser102.

GENERAL STRUCTURE OF *E. COLI* ALKALINE PHOSPHATASE

Alkaline phosphatase exists in the periplasmic space of *E. coli* as a dimer of identical subunits each containing 429 amino acids (11). The four Cys residues are present as two intrachain disulfides. The monomers are synthesized as a preenzyme containing a Leu-rich signal peptide of 22 residues (7, 45, 56, 57). Processing occurs via a signal peptidase after secretion through the membrane (17). Recent data suggest that formation of active enzyme upon dimerization may be a complex process involving some modulator molecules (J. F. Chlebowski, personal communication). A comparison of the amino acid sequences of the phosphorylated peptides isolated from the enzyme with the complete amino acid sequence showed that the phosphorylated residue was Ser102. Figure 1*a* shows the overall shape and polypeptide conformation found in the crystal structure of the dimer. Figure 1*b* shows a ribbon diagram of the secondary structure of the monomer.

SUMMARY OF SUBSTRATE SPECIFICITY AND KINETICS OF ALKALINE PHOSPHATASE

Alkaline phosphatase is thought to be strictly a phosphomonoesterase, although one recent investigation found a low phosphodiesterase activity

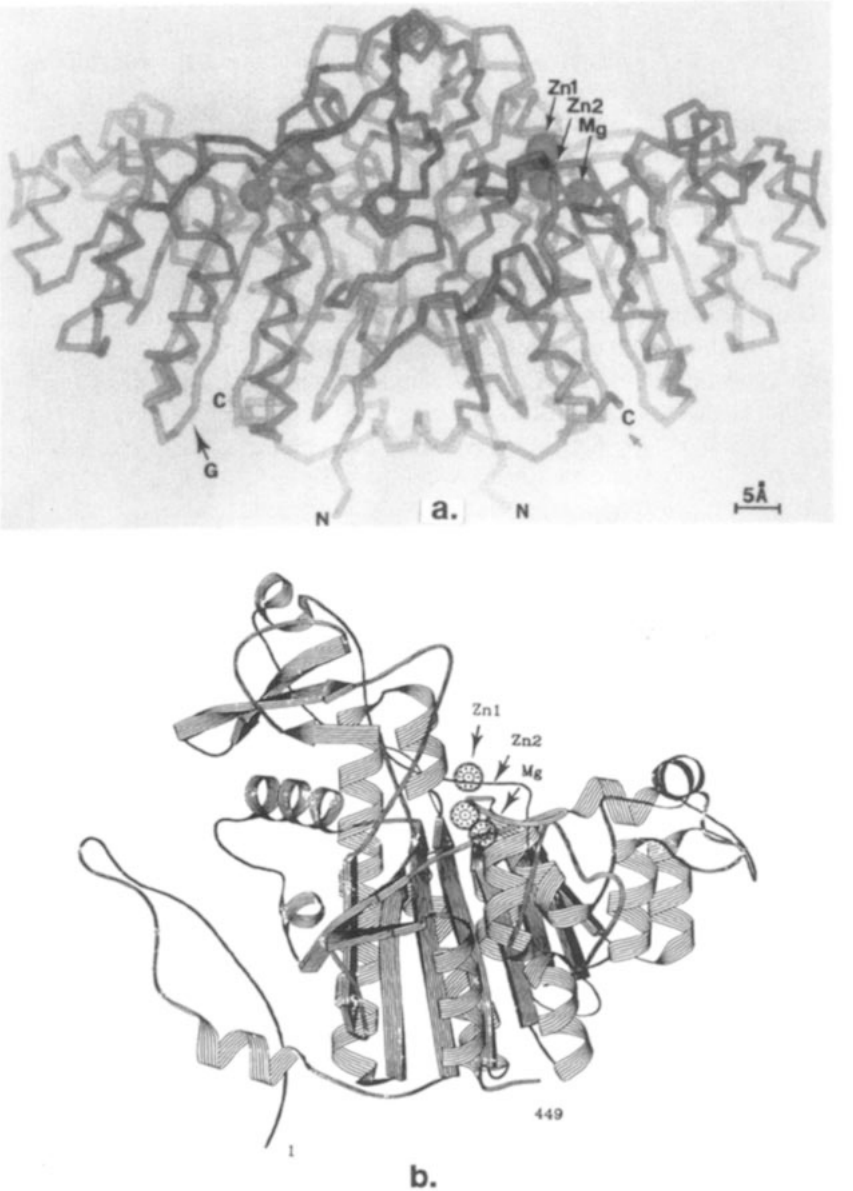

Figure 1 (*a*) Alpha-carbon trace of the dimer of *E. coli* alkaline phosphatase. The non-crystallographic two-fold axis is vertical and the maximum dimension of the dimer is horizontal. The three metal ions at each active center are shown as spheres and the two active sites of the dimer are 30 Å apart. (*b*) Ribbon drawing of the monomer of *E. coli* alkaline phosphatase. The three metal ions are shown as stippled spheres, Zn1, Zn2, and Mg as indicated. The center of the monomer consists of a 10-stranded β-sheet flanked by 15 helices of varying lengths. A second 3-stranded β-sheet and an α-helix form the top of the molecule in this view. Reprinted from Ref. 48.

(J. F. Chlebowski, personal communication). The enzyme hydrolyzes not only oxyphosphate monoesters (23, 29, 41, 63), but also a variety of O- (58, 59) and S-phosphorothioates (19), phosphoramidates (63), thiophosphate, and phosphate (3, 19, 65, 69); hydrolysis of the latter group is reflected by the catalysis of the exchange of ^{18}O from $H_2{}^{18}O$ into inorganic phosphate (3, 65, 69) or the release of H_2S from thiophosphate (19). The enzyme has an alkaline pH maximum, and the rate follows an approximately sigmoid pH-rate profile with an apparent pK_a of ~ 7.5 (19, 34, 50, 63). Table 1 summarizes substrate structure, reaction products, and k_{cat} values. In the case of oxyphosphate monoesters, the k_{cat} is apparently independent of the R group, which can vary from a large protein molecule to a methyl group (63). This finding reflects the fact that either the dephosphorylation of E-P or the dissociation of the product, P_i, is the rate-controlling step depending on pH. A variety of NMR methods have demonstrated that the latter step is rate limiting at alkaline pH (38, 44). In hydrolysis of P_i (^{18}O exchange) or release of H_2S, however, the phosphorylation of Ser102 by the substrate appears to be so slow as to be rate controlling (9, 19, 63).

Alkaline phosphatase reactions can be fit to the general kinetic formulation given in Scheme 1,

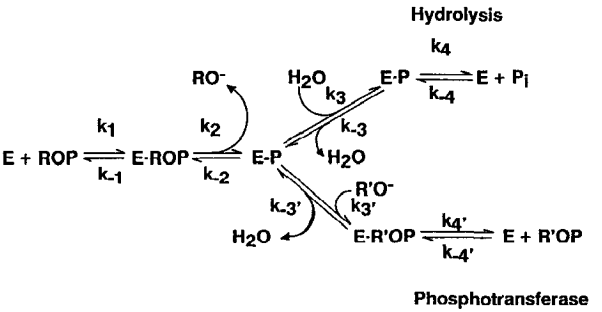

Scheme 1

which includes the covalent phosphoseryl intermediate, E-P, formed when Ser102 is phosphorylated, and the noncovalent complex, E·P, which is formed with the product, P_i. At pH 5.5 and below, the E-P $\rightleftharpoons$ E·P equilibrium favors E-P such that P_i can phosphorylate Ser102 to form high equilibrium concentrations of E-P (for summary, see 63). Scheme 1 also includes the finding that solvent, H_2O, is not the only acceptor for the phosphate from E-P. Almost any alcohol will serve as an acceptor at pH values above 9 and acceptor concentrations near 1 M as shown by recent ^{31}P NMR assays (38). Traditionally, amino alcohols with the amino group

Table 1 Values of k_{cat} for phosphate monoesters hydrolyzed by alkaline phosphatase

Substrate (conditions)		k_{cat}, pH 8.0 (s^{-1})
$ROPO_3^{2-}$	(0.1 M Tris)	8.5[a]
$ROPO_3^{2-}$	(1.0 M Tris)	13–45
$ROPO_3^{2-}$	(1.0 M Tris), Co(II)	≈2
$RSPO_3^{2-}$	(1.0 M Tris)	30
$RNHPO_3^{2-}$	(1.0 M Tris)	28
$ROPSO_2^{2-}$	(0.1 M Tris)	0.005
$ROPSO_{2-}$	(1.0 M Tris)	0.09
$ROPSO_2^{2-}$	(1.0 M Tris), Co(II)	0.17
$HSPO_3^{2-}$		0.26
$HOPO_3^{2-}$		0.15–0.2

[a] When a single k_{cat} is given, it stands for a representative value for substrates that have been the subject of relatively few studies. If a range is given, it reflects a substrate for which a great many values of V_{max} are available in the literature.

on the carbon adjacent to that carrying the accepting OH, e.g. Tris and ethanolamine, have been used to demonstrate this phosphotransferase activity (63). These acceptors not only have enhanced acceptor activity, but show maximum transferase activity around pH 8 (63). The rate rapidly falls off at higher pH values, pH 8–11 (38). Analysis of the high-resolution crystal structure does not as yet suggest the reason for this special reactivity of amino alcohols. The mechanism of the phosphotransferase activity based on a variety of NMR evidence is postulated to involve the co-ordination of the alcoxide ion to one of the zinc ions at the active site instead of a water molecule (38).

Since the original isolation of a phosphorylated serine from alkaline phosphatase by Engström's laboratory (27, 28), kinetic analyses of the enzyme reaction have included steps for the formation and dephosphorylation of the serylphosphate. Rapid-flow kinetic methods applied to examine the initial phases of the hydrolysis of nitrophenyl phosphates by the enzyme revealed that the enzyme produced a relatively rapid burst of phenolate product followed by a steady-state rate at acid pH, but no burst was observed at alkaline pH, where the enzyme was maximally active. The acid burst was readily explained by the finding that dephosphorylation of E-P was very slow, 0.1 s^{-1}, and rate limiting. The possible rate-limiting step at alkaline pH was less clear. The rate of phosphorylation of the serine hydroxyl at pH 5.5, calculated from the burst rate, ranged from 17 to 30 s^{-1} as assembled from numerous studies. In 1973, Bloch & Schlessinger

(8) demonstrated that the rapid-flow kinetics were badly distorted by phosphate that was bound to the native enzyme and carried along through most standard isolation procedures. When phosphate-free enzyme was employed for rapid-flow measurements, they observed instantaneous bursts of RO^- (within the 3-ms dead time of the instrument) at both pH 5.5 and 8.0. The readdition of phosphate abolished the burst at alkaline pH and slowed down the burst rate at acid pH. Thus, contaminating phosphate can abolish the burst at alkaline pH by the prior formation of E·P, but in general cannot completely abolish the burst at pH 5.5, because E-P is not 100% formed. Even more importantly, most stock enzymes were diluted from neutral pH where no E-P was present at the time of mixing. Thus, $HOPO_4^{2-}$ simply competed with $ROPO_4^{2-}$ binding at acid pH. Because phosphorylation from the monoester is so much more rapid than from phosphate, the rate of release of RO^- slowed during the transient phase, despite the fact that the ester still carried out most of the phosphorylation of the enzyme. An important fact emerging from these studies is that phosphorylation from $ROPO_4^{2-}$, even at acid pH, is a much more rapid process than previously believed. Since the bursts at both pH 5.5 and pH 8.0 are instantaneous, k_2, the phosphorylation rate in Scheme 1, must be at least 300 s^{-1} throughout the pH range from pH 5.5 to 8.0 and may be even faster.

The values of many of the kinetic and equilibrium constants describing the alkaline phosphatase reaction (Scheme 1) are plotted in Figure 2 as a function of pH. The pH-rate profile, expressed as k_{cat}, is presented as a sigmoid function corresponding to a single pK_a of 7.5 (Figure 2*a*). After collection of most of the published data on pH-rate profiles for the *E. coli* enzyme, this curve was chosen to represent k_{cat} (see 19, 50, 58, 65). Although not all pH-rate profiles fit the theoretical curve for a single ionization, the most extensive analyses of pH-rate profile data using Dixon plots (log V_{max} vs pH) show that the pH-rate profile can be adequately fit by a single pK_a (50). This finding suggests, but does not prove, that a single proton dissociation is involved. Under conditions usually employed for alkaline phosphatase assays, the pK_a for V_{max} is $\sim$7.5; however, depending on whether neutral buffers, cationic buffers or added organic solvents are present, the apparent pK_a has been observed to vary from 6.58 to 7.55 (50). K_m values for phosphate monoesters remain constant as a function of pH until above pH 8, where an increase in the magnitude of K_m can be fit with an apparent pK_a near 9 (Figure 2b) (50). Thus, V_{max}/K_m plots are bell-shaped if high pH values are included. The increase in K_m at high pH may be connected with a phenomenon of phosphate dissociation at high pH observed using ^{31}P NMR and discussed further below.

Direct measurements of k_3, the rate for dephosphorylation of the phos-

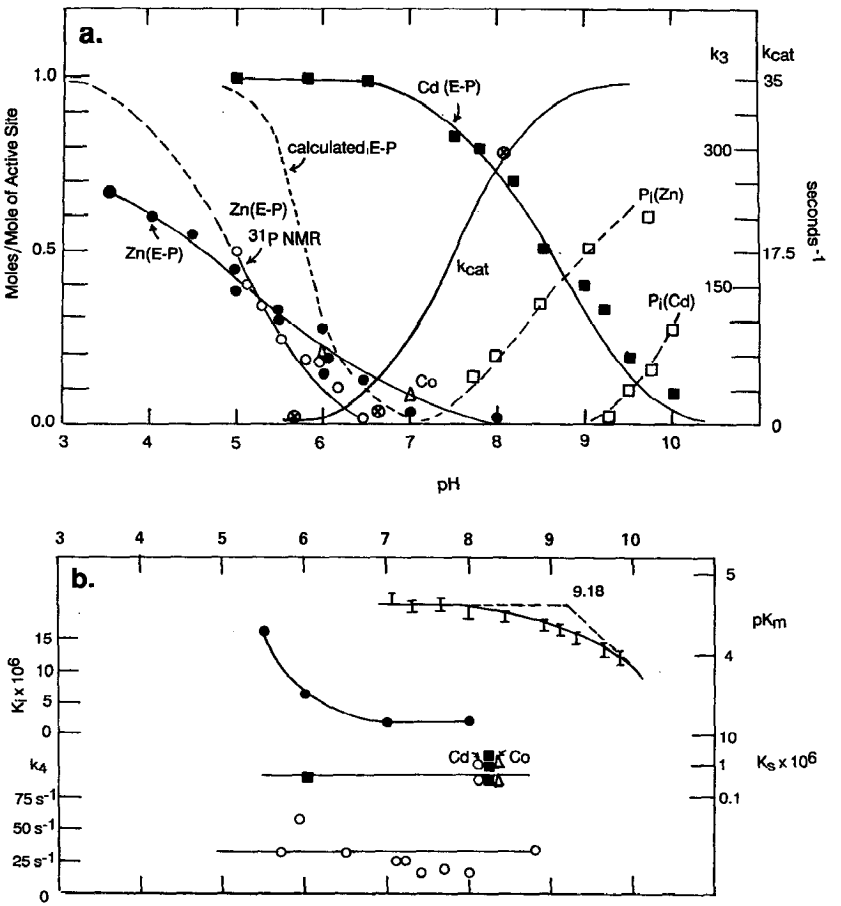

Figure 2 Summary of kinetic constants, equilibrium constants, and concentration of phosphoenzyme intermediates describing the interaction of phosphate monoesters and phosphate with *E. coli* alkaline phosphatase as functions of pH. (*a*) (*Solid circle*) Moles of E-^{32}P formed per mole of active site by the native zinc enzyme. (*Open circle*) E-P per mole of active site as determined using ^{31}P NMR. (*Dashed line*) Expected moles of E-P formed per mole of active site calculated from kinetic constants (52). (*Solid square*) E-P formed by Cd_6AP per mole of active site as determined by labeling with $H^{32}PO_4^{2-}$ and using ^{31}P NMR. (*Open triangle*) E-^{32}P formed by CoAP. (*Solid line*) The central sigmoid curve labeled k_{cat} represents the pH-profile of k_{cat} (see text). (*Circled X*) k_3, value for the desphosphorylation rate of E-P determined as described in the text. (*Open square*) P_i (moles per mole of active site) dissociating from the $Zn_4Mg_2^-$ and Cd_6 alkaline phosphatase; at acid pH, both enzymes bind 2 mol of phosphate per mole of dimer. (*b*) (I) K_m for hydrolysis of $ROPO_4^{2-}$. (*Solid circle*) K_i for inhibition of $ROPO_4^{2-}$ hydrolysis by phosphate. K_s represents equilibrium constants for $^{32}P_i$ binding to AP as determined by equilibrium dialysis for the Zn (*solid sqaure*), Cd (*open circle*) and Co (*open triangle*) enzymes. (*Open circle*) k_4, dissociation rate of phosphate from E·P as determined using ^{31}P NMR in version transfer.

phoseryl residue (E-P), are difficult to obtain. The relatively few values in the literature are those calculated in order to fit reaction profiles observed in rapid flow kinetics. Because k_{-3}/k_3 = E-P/E·P, many reasonably accurate values of this ratio are available. Estimates of k_3 vs pH taken from kinetic analyses of the alkaline phosphatase reaction are plotted in Figure 2*a*. Because most rapid-flow kinetics studied prior to 1973 were distorted by the presence of contaminating inorganic phosphate bound to the enzyme (8), some modification of the estimates of the magnitude of k_3 are required, especially at alkaline pH. One can determine a lower limit for k_3 from the dead time of the stopped-flow instrument because an instantaneous burst of $\sim$1 mol of RO^- per mole of active site is observed at alkaline pH for the phosphate-free enzyme and because this burst results from the slow, 35 s^{-1}, rate-limiting dissociation of E·P. Therefore, as noted above, k_3 must be $\geqslant$300 s^{-1} at pH 8.0; the scale for k_3 in Figure 2*a* has been adjusted to reflect this.

The equilibrium concentration of E-P (1.0 represents maximum possible formation of phosphoserine) for the Zn, Co, and Cd enzymes has been plotted from data obtained by ^{32}P labeling of the enzyme by incubation with $H^{32}PO_4^{2-} \rightleftharpoons H_2{}^{32}PO_4^-$, followed by manual quenching (3, 65). The curve marked "calculated" is the equilibrium concentration of E-P formed as a function of pH predicted by Wilson and his colleagues from the kinetic constants for the E-P$\rightleftharpoons$E·P$\rightleftharpoons$E+P_i reaction as assembled from the extensive kinetic data (52). These investigators suggested that the reason the predicted curve is steeper than the observed values obtained from several laboratories using ^{32}P labeling is the difficulty of quenching the enzyme rapidly enough to trap all the phosphoserine.

The E-P$\rightleftharpoons$E·P equilibrium vs pH also has been determined using ^{31}P NMR to avoid perturbing the equilibrium by the method of detection. The ^{31}P NMR of the enzyme-bound phosphate can quantitate these two intermediates from pH 10 to 5. Between pH 7 and 10, no detectable E-P is present at equilibrium. Between pH 7 and 5, the ratio of E-P/E·P rises along a sigmoid curve and reaches a value of 1 at pH 5. Below pH 5, the zinc enzyme is unstable. Because the ratio is determined accurately by ^{31}P NMR at close intervals over half the pH function, one can extrapolate a sigmoid function for the E-P/E·P ratio with a midpoint at pH 5 as shown in Figure 2*a*. Values of k_4 for dissociation of P_i remain relatively constant from pH 5.7 to 8.8 as determined using ^{31}P NMR inversion transfer (Figure 2*b*) (Table 2) (38). Values of the equilibrium constant for phosphate binding, K_s, as determined by equilibrium dialysis using $H^{32}PO_4^{2-}$ are shown for pH 6 and pH 8.8, the latter for the Zn, Co, and Cd enzymes (3). For the Zn enzyme, K_i values for phosphate kinetically determined by Wilson's laboratory are shown for pH values of 5.5, 6.0, 7.0, and 8.0 (52).

Table 2 Dissociation rates of the product, inorganic phosphate, from the active site of alkaline phosphatase as a function of the metal ion composition of the enzyme[a]

Enzyme	k_{off} (s^{-1})
$Zn(II)_4AP$ (pH 8.8)	35
$Zn(II)_4AP$ (pH 5.7)	33
$Zn(II)_4AP$ + 1.0 M Cl^- (pH 8.0)	60–260[b]
$[Zn(II)_AMg(II)_B]_2AP$ (pH 8.0)	≈1
$[Zn(II)_AMg(II)_B]_2AP$ + 0.1 M Cl^- (pH 9.0)	1.8
$[Zn(II)_AMg(II)_B]_2AP$ + 1 M Cl^- (pH 9.0)	≈15
$[Zn(II)_ACd(II)_B]_2AP$ (pH 9.0)	≈2
$Cd(II)_6AP$ (pH 9.0)	<1
$Cd(II)_6AP$ + 1 M Cl^- (pH 9.0)	≈10

[a] All samples were in 0.01 M Tris-acetate (38).
[b] Too fast to measure directly by ^{31}P NMR inversion transfer; limits given are based on the inversion transfer measurement at 162 MHz.

The value of k_3, the dephosphorylation rate of E-P, falls rapidly from pH 8.0 ($\geq 300\ s^{-1}$) to pH 6.3 ($\sim 1.3\ s^{-1}$), over the same pH range in which k_{cat} falls by ~90% (Figure 2*a*). Thus, the pH-rate profile (from alkaline to acid pH) is coincident with a change in the rate-limiting step from phosphate dissociation to dephosphorylation of the phosphoserine. At pH 8, k_3 exceeds the rate of dissociation of the product phosphate, k_4, by ~10-fold. At pH 6.3, however, the relationship is reversed; k_4 is 26-fold faster than k_3 and is no longer rate limiting. On the other hand, k_3 is not yet as slow as k_{-3}, the rate of phosphorylation of Ser102 from E·P, and thus significant equilibrium concentrations of E-P are not observed at pH 6.3. At pH 5, k_3 has decreased further such that $k_3 = k_{-3}$ and [E-P] = [E·P] at equilibrium (Figure 2*a*). Judging by ^{18}O exchange experiments, both constants must be on the order of 0.1 s^{-1}. The possible identity of the $AH \rightleftharpoons A^- + H^+$ equilibria governing k_3 and the pH-rate profile are discussed in the section on structure and mechanism.

Phosphate is both a substrate and competitive inhibitor of the enzyme. Phosphate binding appears to be essentially pH independent between pH 5.5 and 8.0 if the values for K_i and K_s are taken as a guide (Figure 2*b*) (3, 52, 63). In support of this conclusion is the fact that the dissociation rate of inorganic phosphate from the enzyme, k_4, is also pH independent from pH 5.5 to 8.8 (38). A pH independence of phosphate binding to alkaline phosphatase is surprising because two proton dissociations of phosphoric acid may fall in the pH range 5 to 10, $H_2PO_4^- \rightleftharpoons HPO_4^{2-} + H^+$ ($pK_a = 6.8$) and $HPO_4^{2-} \rightleftharpoons PO_4^{3-} + H^+$ (normal $pK_a \approx 12$). The latter could affect the

AP-phosphate equilibrium if E·P forces formation of the trianion as some reasoning suggests (see below). An enzyme active center, which excludes all but specific water molecules, may limit proton access from the bulk solvent as well. Even in the apophosphoryl enzyme, which is formed by removing Cd from the E-P form of the enzyme, the ^{31}P chemical shift shows that the dianion form of the phosphoseryl group is not titrated to become the monoanion until below pH 4.0 after the enzyme unfolds (34).

At variance with the kinetic constants that suggest that phosphate binding is pH independent is the observation, made using ^{31}P NMR, that while Zn_4AP remains saturated with phosphate to pH 7.0, above pH 7.0 bound phosphate significantly decreases such that $[E\cdot P] = [P_i]$ at pH 10 (Figure 2*a*) when enzyme is 2 mM and phosphate 4 mM (33). The latter finding appears paradoxical, since the measurement of k_4 by NMR inversion transfer shows that the dissociation rate remains constant at $\sim 35\ s^{-1}$ under the same conditions and over the same pH range (Figure 2*b*). While one could postulate that the "on" constant for phosphate binding changes at high pH, this seems unlikely. If a water molecule on Zn_A becomes Zn-$^-$OH at alkaline pH, phosphate binding will compete with hydroxide binding to Zn_A. In support of this postulate is the observation that phosphate does not begin to dissociate from the cadmium enzyme until well above pH 9.0 (Figure 2*a*) (33). However, if both bound phosphates on the enzyme were competing equally with $^-$OH, then k_4 should increase as it does in the case of Cl^- competition (Table 2). One possible explanation of this paradox is negative cooperativity of phosphate binding, i.e. phosphate at one active site is bound less tightly than at the other at pH values above 7.0. Then most of the remaining E·P will be at the tight binding site and the inversion transfer will be weighted in favor of this site.

Negative cooperativity has not been discussed thus far in this review. The phenomenon formed a significant part of earlier discussions of the alkaline phosphatase reaction because many early experiments measuring $H^{32}PO_4^{2-}$ binding or burst magnitude showed that only a single bound phosphate per dimer or a single active site was phosphorylated. When sample-preparation techniques were changed such that samples with a full complement of metal ions were prepared, two E-P or two E·P complexes per dimer were easily formed under most conditions, especially at pH values below 7. Note that the Cd_6AP retains 1 mol of E-P per active site or 2 mol/dimer until the pH rises above 7.0 (Figure 2*a*). From pH 7 to 9, the sum of E-P+E·P also remains 2/dimer for the Cd_6 enzyme (32). Likewise, when enzymes uncontaminated with phosphate were employed in rapid-flow experiments, most burst stoichiometries approached 2/dimer (8).

Before we discard negative cooperativity in alkaline phosphatase as an

artifact, however, I must point out that in the alkaline pH range several sensitive NMR techniques can detect unequal binding constants for the two enzyme-bound phosphates. Detailed ^{31}P NMR titrations of the Zn_4AP and the Cd_6AP with P_i show that at pH 6 both enzymes titrate linearly the formation of 2 mol of enzyme-bound phosphate per mole of dimer. The Cd_6AP does the same at pH 8, but the Zn_4AP titrates the formation of only 1 mol of E·P under the NMR conditions employed (33). The same phenomenon is apparent when phosphate binding to the enzyme is evidenced by ^{35}Cl line broadening resulting from the binding of two $^{35}Cl^-$ ions to each Zn_A. At pH 6, the phosphate ions displace one chloride from each Zn_A site, i.e. half the Cl^-. In contrast, at pH 8 one phosphate displaces only one quarter of this Cl^- in a stoichiometric fashion; displacement of the other quarter requires up to six phosphates per dimer (37). Thus, inequivalent phosphate binding affinities may be involved in product release.

The rate-limiting phosphate product dissociation accounts for burst kinetics observed at alkaline pH by stopped-flow methods when a phosphate-free enzyme is employed (5, 20). Because the enzyme does not appear to recognize the R group of a phosphomonoester, researchers have often assumed that phosphate ester binding affinity was similar to that of phosphate. Indeed, the best measurement of K_m values have been $\sim 10^{-6}$ M for $ROPO_3^{2-}$, although they increase to almost 10^{-4} M for an O-phosphorothioate, $ROPSO_2^{2-}$ (19, 58). When an acceptor alcohol is present, the rate of the phosphotransferase activity is always additive to that of the initial phosphohydrolase as has been confirmed using accurate ^{31}P-NMR measurement techniques (38). Because the dissociation of P_i is rate limiting for the hydrolysis reaction under these conditions, the dissociation of the new product ester in the transferase reaction is clearly considerably more rapid than phosphate dissociation. K_m varies as a function of the metal-ion species, Zn or Co, at the active center (19), but the K_i for phosphate is rather similar for the Zn, Co, and Cd enzymes [$(0.75 \pm 0.25) \times 10^{-6}$ M] (3). If the dissociation rate constant for $ROPO_3^{2-}$ were $\sim 35\ s^{-1}$ as it is for phosphate, then K_m would not represent k_{-1}/k_1, since the phosphorylation rate at pH 8 is at least $10^2\ s^{-1}$ and probably even faster.

In comparing the kinetic pattern observed for phosphate esters as substrates and the information derived from using phosphate as substrate to form E-P, one should keep in mind that phosphorylation of the enzyme by $HOPO_3^{2-}$ has become rate-limiting, as concluded from the fact that the ^{18}O exchange rate, 0.1 to 0.2 s^{-1}, is slower than the dephosphorylation of E-P over most of the pH range and is always slower than the dissociation of P_i. The ^{18}O exchange reaction is pH independent, evidence that the apparent pK_a reflected in the normal pH-rate profile is that of a group

primarily affecting a step following formation of the phosphoseryl intermediate (see below). This pH independence, presumably controlled by a slow phosphorylation, is confirmed by the hydrolysis of thiophosphate, which releases H_2S (19). The rate of release of H_2S from thiophosphate is the same at pH 5.5 and 8.0 and is only slightly more rapid than the rate of ^{18}O exchange into phosphate catalyzed by the enyzme (Table 1).

The above background is useful in considerations of the nature of the transition state in the alkaline phosphatase mechanism and whether the reaction is primarily associative via the initial attack of the Ser-O^- on the phosphorous or whether the enzyme mechanism involves significant dissociative features via activation of the leaving group as in non-enzyme-catalyzed phosphomonoester hydrolysis (6, 49, 78). Recent investigations have probed this question and confirmed that k_{cat}/K_m values for a variety of substrates as functions of the pK_a of the leaving group show β values of ~ 0.1 rather than the value of ~ 1 expected for a dissociative reaction (51, 78). Although these newer findings and earlier, less rigorous kinetics have been interpreted to mean that the enzyme mechanism is purely nucleophilic in character, forming a five-coordinate intermediate, the high resolution crystal structure of E·P reveals interesting structural arrangements of metal and phosphate that bear on this view of the mechanism, as discussed in the next section of this perspective.

Using the phosphotransferase reaction to capture as a second chiral phosphate ester the phosphate from E-P initially formed by a chiral phosphomonoester containing ^{16}O, ^{17}O, and ^{18}O, Jones et al (46) demonstrated that the alkaline phosphatase reaction proceeds with retention of configuration around phosphorus. This result suggested that the reaction path consists of two in-line nucleophilic attacks; the first by the Ser-OH (or Ser-O^-) and the second by solvent H_2O (or ^-OH).

THE METALLOENZYME NATURE OF ALKALINE PHOSPHATASE

The original analytical data reporting that alkaline phosphatase was a Zn metalloenzyme showed two Zn ions per dimer (62). Subsequent determinations of the zinc content by the original laboratory and other investigators showed that with different preparation techniques the Zn:protein dimer ratio was generally 4 and under some circumstances could reach 6 (1, 10, 25, 60). Numerous studies contribute to these conclusions; it is now certain that a fully active native alkaline phosphatase contains four Zn and two Mg ions, the Zn occupying sites designated A and B, while Mg occupies sites designated as C. The A, B, and C sites were first unequivocally demonstrated using ^{113}Cd NMR. The $^{113}Cd_6$ enzyme shows three

NMR signals at 153, 70, and 0 ppm relative to $Cd(ClO_4)_2$, each of which integrates into two Cd ions per dimer (Figure 3) (32, 35). Solution studies suggested that two sites, believed to be the A and B sites as defined from the ^{113}Cd NMR (Figure 3), were filled by Zn in the native protein (1, 10, 25). The crystal structure of the native zinc enzyme confirms the occupancy of sites A and B by Zn and of site C by Mg (48). The signal at 153 ppm is sensitive to conditions resulting from the exposure of this site to the addition of ligands from solution, H_2O, or anions. Thus, the chemical shift, δ, has been observed to vary from 150 to 170 ppm (see below).

Based on what is now known of ^{113}Cd NMR chemical shifts as a function of ligand donor atoms, the shift of 153 ppm, assigned to A-site ^{113}Cd, is compatible with a site containing two His N atoms serving as donors with oxygen atoms as the remaining donors (see crystal structure below). The ^{113}Cd NMR signal at 70 ppm is compatible with assignment to the B site containing one His N, where the rest of the donors are oxygen; while the ^{113}Cd chemical shift of 0 ppm is expected from a site such as the C site, which is composed of all oxygen donors. The variable metal stoichiometry displayed by alkaline phosphatase preparations is readily accounted for because the ammonium sulfate used in practically all preparative pro-

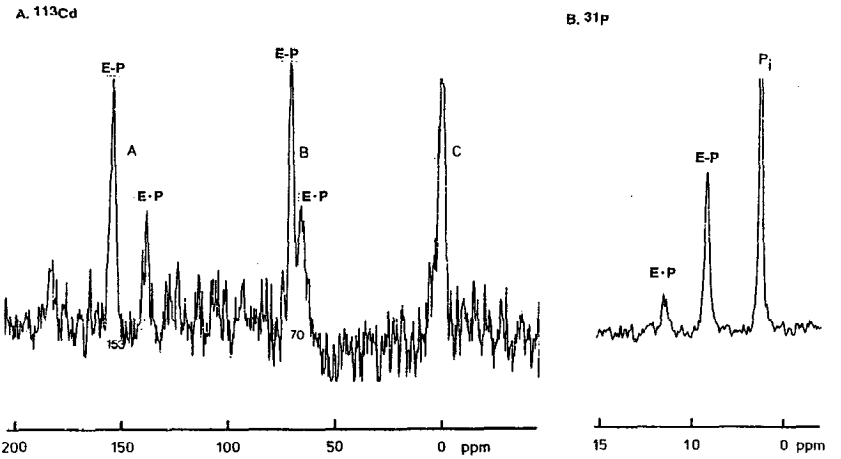

Figure 3 ^{113}Cd NMR (*A*) and ^{31}P NMR (*B*) of $^{113}Cd_6AP$ (3 mM) in 0.01 M Tris HCl, pH 8.3, containing 2 mol of bound phosphate in the presence of equimolar free P_i (^{31}P $\delta = 3$ ppm). At pH 8.0, ~80% of the enzyme is present as E-P (^{31}P $\delta = 8.7$ ppm), and ~20% is present as E·P (^{31}P $\delta = 13.0$ ppm). The ^{113}Cd signals at 153 and 70 ppm reflect the ^{113}Cd ions in sites A and B for an enzyme in the E-P form, while the small peaks, 20 and 8 ppm upfield respectively, are the signals from the A- and B-site ^{113}Cd of an enzyme in the E·P form. Data are from Ref. 32.

cedures can easily remove Zn from the B site as well as from the A site at high pH. In fact, the best way to prepare the apoenzyme is to dialyze the enzyme at pH 9 against buffered 2 M ammonium sulfate (33).

The relationship between occupancy of the three metal-ion binding sites, A, B, and C, on each monomer and phosphatase activity was not an easy one to define, but required enzymes with known metal : protein stoichiometry as well as knowledge of which sites were occupied (33, 34, 38). Mixed-site occupancy occurs easily when metal ions are present at less than full stoichiometry. While a $(Zn_AZn_BMg_C)_2$ enzyme has maximal activity, an enzyme containing only two Zn ions, one at each A site, is not inactive. Such a two-Zn enzyme binds phosphate and catalyzes phosphorylation of Ser102 (2). In fact, if Mg occupies both the B and C sites, the activity of the $(Zn_AMg_BMg_C)_2$AP is near normal in the phosphotransferase reaction (Table 3) (21). In contrast, the normal hydrolysis reaction is much depressed in the $(Zn_AMg_BMg_C)_2$AP (Table 3) (21, 38). Because standard

Table 3 Effect of metal-ion species on the E-P $\rightleftharpoons$ E·P equilibrium at the active center of alkaline phosphatase (AP) and the k_{cat} values

Metal site occupancy at active center	k_{cat} s^{-1}	pH at which [E-P] = [E·P][a]	^{31}P chemical shift, ppm	
			E-P	E·P
$[Zn(II)_AZn(II)_B]_2$AP	35	5.0	8.6	4.3
$[Zn(II)_AZn(II)_BMg(II)_C]_2$AP	35	5.0	8.6	3.4
$[Zn(II)_AMg(II)_B]_2$AP (0.01 M Tris)	1	4.0	8.5	1.8
$[Zn(II)_AMg(II)_B]_2$AP (1 M Tris)	30	—	—	—
$[Zn(II)_ACd(II)_B]_2$AP	2	6	8.0	12.6
$[Cd(II)_ACd(II)_B]_2$AP	0.001[b]	10	8.4	13.4
$[Cd(II)_ACd(II)_BCd(II)_C]_2$AP	<0.1[c]	8.7	8.7	13.0
$[Cd(II)_AZn(II)_B]_2$AP (unstable)	—	7	9.3	
ApoPhosphorylAP	—	—	5.8	
$[Co(II)_ACo(II)_B]_2$AP	2	≈ 5[d]	ND[e]	
$[Mn(II)_AMn(II)_B]_2$AP	0.2[c]	≈ 6.5[d]	ND	

[a] These values were determined from ^{31}P-NMR of the enzyme vs pH unless otherwise indicated.

[b] This is the rate of phosphorylation from E·P taken from the NMR experiment shown in Figure 7. Since the major intermediate accumulating at pH 8 is E-P, dephosphorylation of E-P, k_3, cannot be faster. Thus the turnover, k_{cat}, cannot be faster than 0.001 s^{-1}.

[c] The lower limit for turnover determined by the standard colorimetric assay; i.e. it represents the background from zinc contamination of the best apoenzyme preparations assayed in metal-free buffers and substrates. The value 0.2 s^{-1} is readily detected above the apoenzyme background under metal-free assay conditions (64).

[d] Taken from ^{32}P labeling data (3).

[e] Not detected due to line broadening by the paramagnetic metal ions. Data are from Ref. 16 and 66. Assays were at pH 8, 0.01 M Tris unless otherwise stated.

assays employ 1 M Tris buffer, this difference is not routinely detected. Surprisingly, a large activation of the hydrolysis+transferase reaction by Mg is only observed for the two-Zn species; Mg occupancy of the C site in a 4-Zn enzyme, $(Zn_AZn_{B-C})_2AP$, enhances total activity relatively little if at all. In all the studies of *E. coli* alkaline phosphatases of defined metal-ion stoichiometry, detecting significant effects of the C-site metal ion on structure or function has proved difficult. This statement may not apply to the mammalian enzymes, which undergo much more dramatic activation by Mg even when maximum Zn ions are present (22).

The above brief introduction to the properties of alkaline phosphatase is intended only to set the background for the main purpose of this perspective, which is an attempt to synthesize the findings of the recent 2.0-Å crystal structure of the enzyme and its two phosphoenzyme intermediates with the extensive solution data bearing on the catalytic mechanism of alkaline phosphatase. The resultant synthesis gives the clearest picture yet of the active center and the intermediates on the reaction path of alkaline phosphatase. For detailed descriptions of the earlier kinetic, spectroscopic, and other physicochemical studies of the enzyme, earlier reviews should be consulted (23, 34, 63).

COORDINATION CHEMISTRY AT THE ACTIVE CENTER OF ALKALINE PHOSPHATASE

The coordination chemistry at the active center of alkaline phosphatase is best presented by a detailed description of the structure around each of the three metal ions at the active center of the native enzyme that has the metal composition $Zn_AZn_BMg_C$. Multinuclear NMR investigations of the enzyme done in the past have used the designations A, B, and C for the three sites; the crystal structure uses the designations 1, 2, and 3. Figure 4*a* presents the general structure of the active center by a stereo view of the immediate region of the active center including the three metals (48). Figure 4*b* shows a computer-graphics representation of the E·P complex of the native Zn_4Mg_2 enzyme that includes the metal-ligand bonds, the slowly exchanging water molecules, the hydrogen bonds, and the amino acid side chains located within the immediate region of the active center (48). Both representations are taken from the structure of the E·P complex, i.e. with phosphate bound noncovalently at the active center by soaking crystals of the $(Zn1Zn2Mg3)_2AP$ in phosphate at neutral pH. This structure has been determined at 2-Å resolution and all information suggests it should represent the authentic E·P intermediate. The three metal ions form a cluster in which the metal-to-metal distances trace a triangle of 3.94 × 4.88 × 7.09 Å. Table 4 lists the metal-metal distances, the ligands

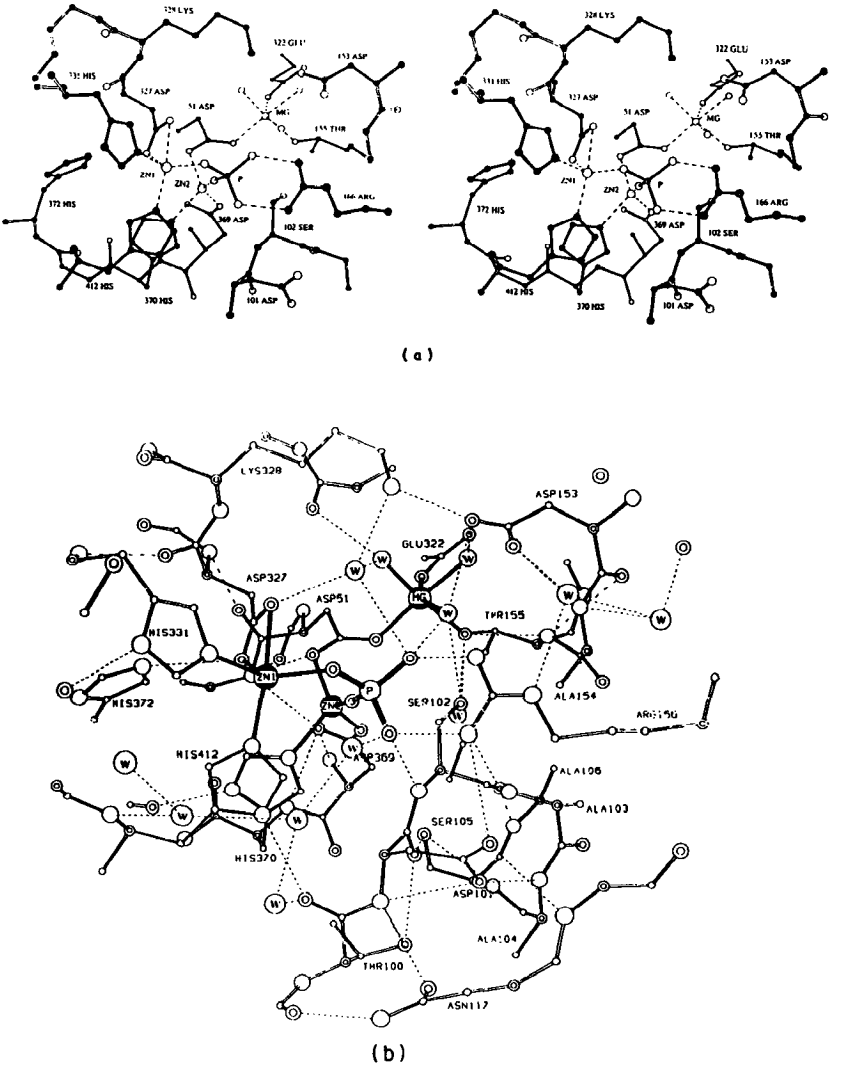

Figure 4 (*a*) Stereo drawing of the active site of the *E. coli* alkaline phosphatase, $(Zn1Zn2Mg3)_2AP$ plus 2 mM HPO_4^{2-}, pH 7.5. Atoms are shaded by atom type. Some residues and water molecules are omitted for clarity. (*b*) The active-site region of the E·P complex (2-Å resolution) including all the atoms within 10 Å of the phosphorus atom. Water molecules are labeled *W*. Hydrogen bonds are shown as broken lines.

Table 4 Summary of the metal-metal and metal-ligand distances (Å) for the dimer of $(Zn1,Zn2,Mg3)_2$alkaline phosphatase[a]

		Distances (Å)	
Metal to metal	Atom	Subunit A	Subunit B
Zn1–Zn2		3.94	4.81
Zn2–Mg		4.88	4.66
Zn1–Mg		7.09	7.03
Metal-ligand			
	Zn1 coordination		
Asp327	OD1	2.00	2.26
	OD2	2.30	2.53
His331	ND1	1.96	2.07
His412	NE2	2.04	2.04
PO_4	O1	1.97	2.12
	Zn2 coordination		
Asp51	OD1	2.13	2.03
Asp369	OD1	1.79	1.80
His370	ND1	2.05	2.01
PO_4	O2	1.97	2.23
	Mg coordination		
Asp51	OD2	2.07	1.96
Thr155	OG1	2.15	2.05
Glu322	OE1	2.26	1.93
Water	O	2.03	1.92
Water	O	1.90	2.00
Water	O	2.32	2.03

[a] The data are taken from Ref. 48.

for each site, and the metal-ligand bond lengths. These distances vary slightly, as observed in the separate monomers, A and B, related by the two-fold axis of the dimer, but the significance of these differences is not clear at present.

The active center is located at the carboxyl end of the central β-sheet, and one monomer provides all the ligands to the three metal ions. The electron-density map of E·P is well defined except for the disordered hydroxyl group of Ser102 (see below). Despite the close packing of the metal centers, there is only one bridging ligand, the carboxyl of Asp51, which bridges between Zn2 and Mg3 or Cd2 and Cd3 in the Cd_6 enzyme. Figure 5 diagrams the coordination around Zn1, Zn2, and Mg3 as it exists in the E·P complex.

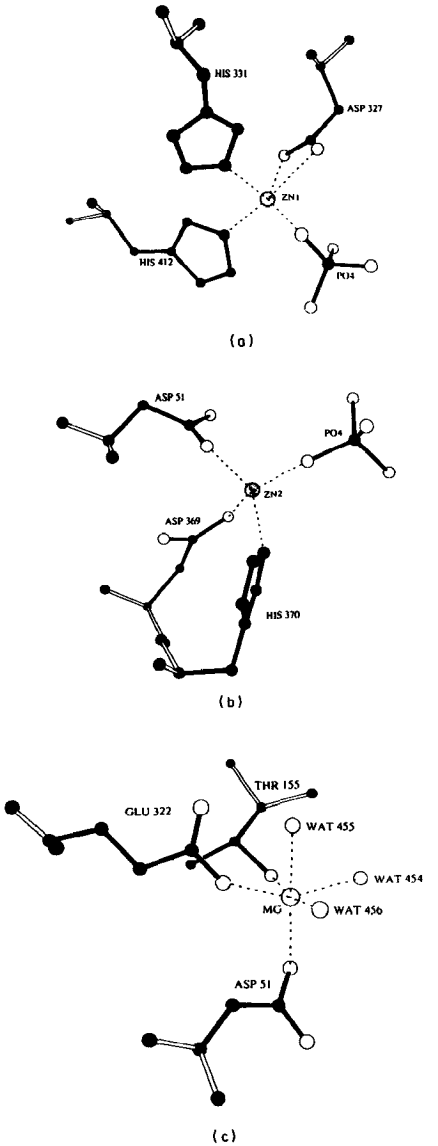

Figure 5 Coordination spheres of the three metals in the E · P complex of $(Zn1Zn2Mg3)_2AP$: (*a*) Zn1, (*b*) Zn2, and (*c*) Mg. Conditions as in Figure 4. The figure is reproduced from Ref. 48.

Zn1(A) Coordination

The A site or Zn1, which upon substitution with first-transition metal ions shows spectroscopic properties of a typical Zn(II) metalloenzyme (2, 34), has four ligands from the protein, which include both carboxyl oxygens of Asp327, the N3 of His331, and the N3 of His412. In the absence of HPO_4^{2-}, water relaxation data (64) and $^{35}Cl^-$ NMR data (37) suggest that the coordination sphere of the A site is completed by two H_2O molecules. In the E·P complex, one of the phosphate oxygens forms a typical coordinate bond with Zn1, with a Zn1-O bond length of 1.97 Å and a Zn-O-P bond angle of 120° (Figure 5*a*). Water-relaxation data using the Mn enzyme show that one of the water molecules coordinated to the A-site metal is displaced by phosphate (64). ^{35}Cl NMR reveals a similar displacement of a monodentate ligand at A-site, i.e. Cl^-, by phosphate binding to the Zn enzyme (37). The Zn1 coordination in E·P can best be described as pseudotetrahedral, where both carboxyl oxygens of Asp327 occupy one of the apices. His372, which was originally thought to coordinate Zn1, is not a direct ligand; it is 3.8 Å away from Zn1, and the N3 of the imidazole ring forms a hydrogen bond with one of the coordinated carboxyl oxygens of Asp327 (Figure 4*b*).

Zn2(B) Coordination

In the E·P complex, Zn2 is coordinated tetrahedrally by the N3 of His370, one of the carboxyl oxygens of the bridging Asp51, and one of the carboxyl oxygens of Asp369 (Figure 5*b*). The tetrahedral coordination is completed by one of the phosphate oxygens. While the Zn2-O bond length is 1.97 Å, identical to that for the Zn1-O bond, the Zn2-O-P bond angle is nearly linear (175°). The OH of Ser102 is disordered in the E·P complex but appears to form a coordinate bond with Zn2 in the phosphate-free enzyme (see below).

Mg3(C) Coordination

The Mg site can be described best as a slightly distorted octahedron consisting of the second carboxyl oxygen of the bridging Asp51, one of the carboxyl oxygens of Glu322, and the hydroxyl of Thr155, while the rest of the coordination sites are filled by three slowly exchanging water molecules (numbered 454 to 456) (Figure 5*c*). Asp153 is not a direct ligand as orginally believed (68, 80), but is an indirect ligand in that the carboxyl group forms hydrogen bonds with two coordinated water molecules (454 and 455) that are the direct ligands to Mg (Figure 4*b*). The Mg site

does not appear close enough to participate directly in the hydrolysis mechanism, but could of course contribute to the shape of the electrostatic potential around the active center (see below).

Enzyme-Bound Phosphate in the E·P Intermediate

Because the relationship between the amino acid side chains and the phosphate in the E·P intermediate forms the basis for the initial discussion of the relationship of the crystal structure to solution studies of the mechanism, additional details of the structure are outlined here. In addition to oxygen-metal bonds to Zn1 and Zn2 made by two of the oxygen atoms of phosphate, the other two phosphate oxygens in E·P hydrogen bond to the guanidinium group of Arg166 (Figure 4*a*). Figure 6*a* shows the electron density map on which this structure is based. The guanidinium group is involved in an additional hydrogen-bond network that includes hydrogen bonds to Asp101 and a water molecule (Wat459), the latter held by Asp153 and possibly also by Tyr169. Of the two phosphate oxygens involved with the guanidino group, one is further hydrogen bonded to the amide of Ser102, and the second seems to be involved with two of the slowly exchanging water molecules. One of these molecules (Wat454) is coordinated to Mg, while the second (Wat457) forms a bridge between the phosphate oxygen and Lys328 (Figure 4*b*). Zn1, O1, P, O2, and Zn2 are nearly coplanar.

Enzyme-Bound Phosphate in the E-P Intermediate

As shown in Figure 2, the substitution of Cd for Zn shifts the pH stability of the covalent phosphoryl enzyme well into the alkaline pH range. Ser102 of the Cd_6 enzyme remains 90% phosphorylated at pH 7.5; hence, crystals of the Cd_6 enzyme when soaked in phosphate can be used to determine a structure of the E-P intermediate. The electron density map at 2.5-Å resolution of the E-P intermediate formed by Cd_6AP is shown in Figure 6*b* and should be compared to the electron density map of the E·P complex of the Zn_4Mg_2 enzyme at 2-Å resolution shown in Figure 6*a*. An ester bond between the phosphate and the hydroxyl of Ser102 is clearly present. Cd2 also appears to form a coordinate bond with the ester oxygen. The phosphate group has moved slightly deeper into the active-center cavity, and whether an oxygen of the phosphate remains close enough to Cd1 to retain a coordinate bond is difficult to determine from the electron density alone (see discussion of mechanism below). The two hydrogen bonds between phosphate oxygens and the guanidino group of Arg166 are maintained in the E-P complex.

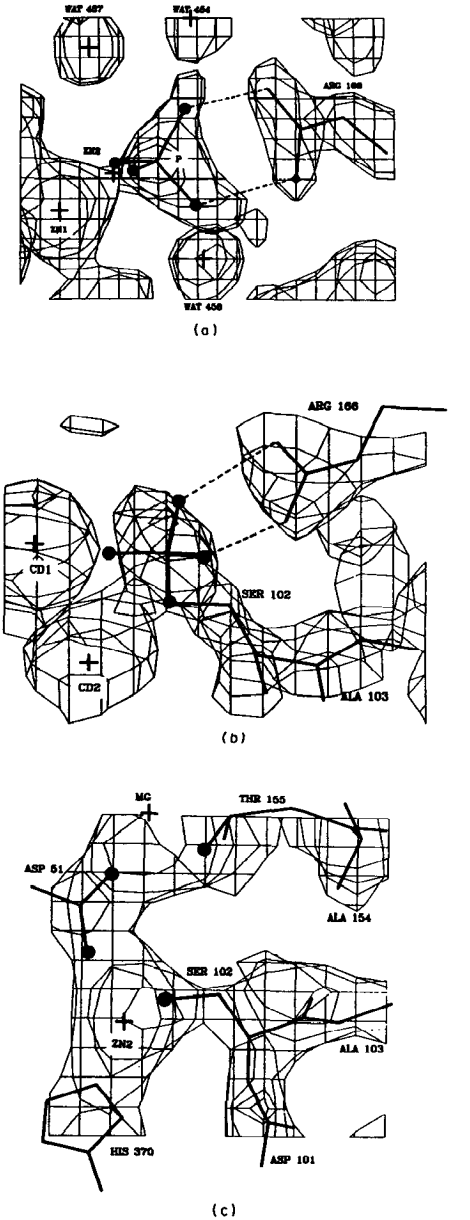

Figure 6 (*a*) $2F_o$-F_c electron-density map of the active-site region of $(Zn1Zn2Mg2)_2AP$ as the E·P phosphoenzyme intermediate. (*b*) Electron-density map of Cd_6AP plus 2 mM HPO_4^{2-}, pH 7.5; atoms within 8.0 Å of Ser102 are omitted from the structure factor and phase calculations. The final refined model is superimposed on the density map. (*c*) Electron-density map of $(Zn1Zn2Mg3)_2AP$, pH 7.5, in the absence of phosphate; atoms within 8.0 Å of Ser102 are omitted in the calculation of the structure factor and phases. The final refined model is superimposed on the density map. The figure is reproduced from Ref. 48.

CHANGES IN ACTIVITY OF ALKALINE PHOSPHATASE ON SUBSITUTING CADMIUM, COBALT, OR MANGANESE FOR THE NATIVE ZINC ION

The substitution of the native Zn ions in sites A(1) and B(2) with other first transition or IIB metal ions significantly changes k_{cat} as well as the rate constants for individual steps. While the structural reasons for all these changes are not immediately obvious, the results have been helpful in understanding specific aspects of the mechanism.

The most dramatic change is the fall in k_{cat} upon Cd substitution from $\sim 35\ s^{-1}$ to a rate impossible to detect using standard assay techniques. Both ^{32}P labeling at low pH and NMR detection of E-P and E·P, however, show that the Cd enzyme forms both of these phosphoenzyme intermediates. Inversion transfer from $^{31}P_i$ to the E·^{31}P complex on the Cd_6 enzyme show that k_4, the dissociation of the product phosphate, has slowed to less than $1\ s^{-1}$ as a result of the Cd substitution (Table 2). The dissociation of phosphate, however, is no longer the rate-limiting step for the Cd enzyme. By following the formation of E-P via observation of its ^{31}P NMR resonance, the phosphorylation rate of the cadmium enzyme from $HOPO_3^{2-}$, k_{-3}, is $\sim 10^{-3}\ s^{-1}$ at pH 9.0 (see Figure 7 below). Over much of the pH range, however, k_3, the dephosphorylation of E-P, must be even slower because the major equilibrium species of intermediate is E-P until the pH is above 9 (Figure 2*a*). One of the possible explanations for the latter remarkable fall in k_3 is that the solvent nucleophile required for the dephosphorylation step is coordinated to the A-site metal, and its pK_a has been shifted far to alkaline pH by the Cd substitution. Although the NMR studies show the Cd enzyme following all the steps of the native enzyme, it is essentially an enzyme in slow motion.

Substitution of Co, on the other hand, causes far less drastic changes. While k_{cat} falls significantly, $2–10\ s^{-1}$ depending on preparation (Table 3) (19), the pH-rate profile for V_{max} remains nearly the same as that for the zinc enzyme, with an apparent pK_a of ~ 7.5 (19). Compatible with this finding is the observation that significant equilibrium concentrations of E-^{32}P form only below pH 7. The acid instability of the Co enzyme prevents determination of the complete pH dependence of the E-P/E·P ratio (3). The Co substitution, however, is accompanied by a dramatic switch in the relative magnitudes of phosphate dissociation, k_4, vs the rephosphorylation rate of Ser102 from E·P, k_{-3}. ^{31}P NMR can be used to accurately measure the exchange of ^{18}O out of $HP^{18}O_4^{2-}$ as catalyzed by alkaline phosphatase, since an isotope shift in the ^{31}P signal is induced proportional to the number of ^{18}O oxygens in the phosphate (9). The exchange catalyzed by the native

Zn(II) enzyme is compatible with a kinetic scheme in which E·P dissociates at least 10 times more rapidly than E-P is reformed, in agreement with the rate constants given above, i.e. $k_4 = \sim 35\ s^{-1}$ (Table 2), while the rephosphorylation rate, k_{-3}, is $\sim 0.2\ s^{-1}$ for Zn. On the other hand, Co(II) catalyzes the exchange of approximately three phosphate oxygens per turnover, showing that several rephosphorylations of the Ser102 occur before E·P can dissociate. The multiple ^{18}O exchanges from E·P catalyzed by the Co enzyme allow the conclusion that E·P is a dynamic complex in which the phosphate oxygens interchange their positions on a reasonably fast time scale, probably between 10 and 100 times per second to accommodate both the ^{18}O exchange data and the k_{cat} observed for the Co enzyme. Although paramagnetic broadening of the bound phosphate by Co(II) prevents the measurement of k_4 for the Co enzyme by the accurate NMR methods, similar equilibrium dissociation constants measured for phosphate binding to the Co and Zn enzymes (3) suggest that the phosphate dissociation rates may be similar. Thus Co appears to catalyze phosphorylation of Ser102 from E·P more rapidly than Zn. While precise explanations of the above phenomena are not possible, even with the 2-Å map of the E·P complex, they do emphasize the close interactions between the phosphate and the metal ions.

Substitution of Mn for Zn produces an enzyme with far less activity, but one that is nevertheless detectable by the standard assays with *p*-nitrophenyl phosphate and estimated to be $0.2\ s^{-1}$ (64). Although very low, the latter is significantly greater than the turnover number for the Cd enzyme. While the kinetics of the Mn enzyme have not been investigated in detail, part of the fall in k_{cat} must reflect a fall in k_3, the dephosphorylation rate of E-P, because significant equilibrium concentrations of E-P are formed by the Mn enzyme at pH 8 and above (3).

CONCLUSIONS ON STRUCTURE AND MECHANISM OF ALKALINE PHOSPHATASE DERIVED FROM MULTINUCLEAR NMR

Investigators used ^{113}Cd NMR of the $^{113}Cd_6AP$ to originally identify the presence of three separate metal-ion binding sites, A, B, and C, on each monomer of alkaline phosphatase (32). The chemical shifts of two of these sites, A and B, depend on which phosphoenzyme intermediate, E·P or E-P, is present (Figure 3), suggesting originally that both Cd_A and Cd_B were near the phosphate binding site as the structure now shows. ^{31}P NMR signals can be detected from both E·P and E-P intermediates and have been valuable probes of the mechanism. The ^{31}P NMR signal of E·P has

provided the demonstration by saturation and inversion transfer that the dissociation of inorganic phosphate, $k_d \approx 35\ s^{-1}$, is the slowest, and therefore the rate-limiting, step in the mechanism (38). The chemical shifts of the ^{31}P NMR resonances of the two alkaline phosphatase intermediates as well as the pH at which [E·P] = [E-P] for each metalloderivative of the enzyme are summarized in Table 3 and suggest several general conclusions.

For the native $(Zn_AZn_BMg_C)_2$ enzyme, E·P has a resonance at 4 ppm, while E-P resonates 8 ppm downfield of phosphoric acid. The chemical shift of the E-P signal is relatively insensitive to the substitution of the various metal-ion species at sites A or B. In marked contrast, the chemical shift of the E·P signal is highly sensitive to the nature of the metal ion in both sites, shifting from the most upfield position of 1.8 ppm in the $(Zn_AMg_BMg_C)_2$AP to 13 ppm in the $(Cd_ACd_BCd_C)_2$AP. This great sensitivity of the δ of E·P to the nature of the metal ion suggested that the phosphate of E·P was coordinated to one or both metal ions. In the case of the $(Cd_ACd_BCd_C)_2$AP, the phosphate of E·P appeared to be coordinated to only one of the active-center ^{113}Cd ions based on the observation that the ^{31}P signal for E·P is a doublet showing a single 30-Hz ^{31}P-^{113}Cd coupling (Figure 7*a*) (33). Heteronuclear decoupling shows that this coupling comes from the A-site ^{113}Cd, a conclusion supported by the disappearance of this coupling in the $(Zn_ACd_B)_2$AP hybrid enzyme (Figure 7*d*) (36). Although the coupling disappears, upon Zn substitution for the A-site ^{113}Cd, the unusual downfield chemical shift of 12.6 ppm is maintained in a $(Zn_ACd_B)_2$ hybrid (Table 3, Figure 7*d*), which leads to the unexpected conclusion that Cd in the B site rather than the A site induces the unusual downfield shift of the E·^{31}P signal. This observation became less surprising when the crystal structure of E·P showed that a second phosphate oxygen is as close to $Zn_B(2)$ as the more normally coordinated oxygen is to $Zn_A(1)$ (Figure 4*b*).

In contrast to the changes in chemical shift of the E·^{31}P signal, the resonance of the phosphoserine, E-^{31}P, remains between 8.6 and 8.4 ppm no matter what metal ions are in the A, B, and C sites (Table 3). Likewise, in heteronuclear-decoupling experiments, no change in the linewidth of the E-^{31}P singlet is observed on irradiation of either the $^{113}Cd_A$ or $^{113}Cd_B$ signals. These characteristics of the phosphorous nucleus in the E-P complex led to the suggestion that at least on the appropriate NMR time average, the phosphate of E-P is not coordinated to either A-site or B-site metal ions. However, if the $Cd_B(2)$ is coordinated to the ester oxygen as the electron density map suggests, a ^{113}Cd-O-^{31}P coupling may not be resolved. The structure in the immediate vicinity of the phosphoseryl-102 is significantly influenced by the metal ions, since removal of the Cd ions from the E-P form of the Cd_6 enzyme results in an apophosphoseryl

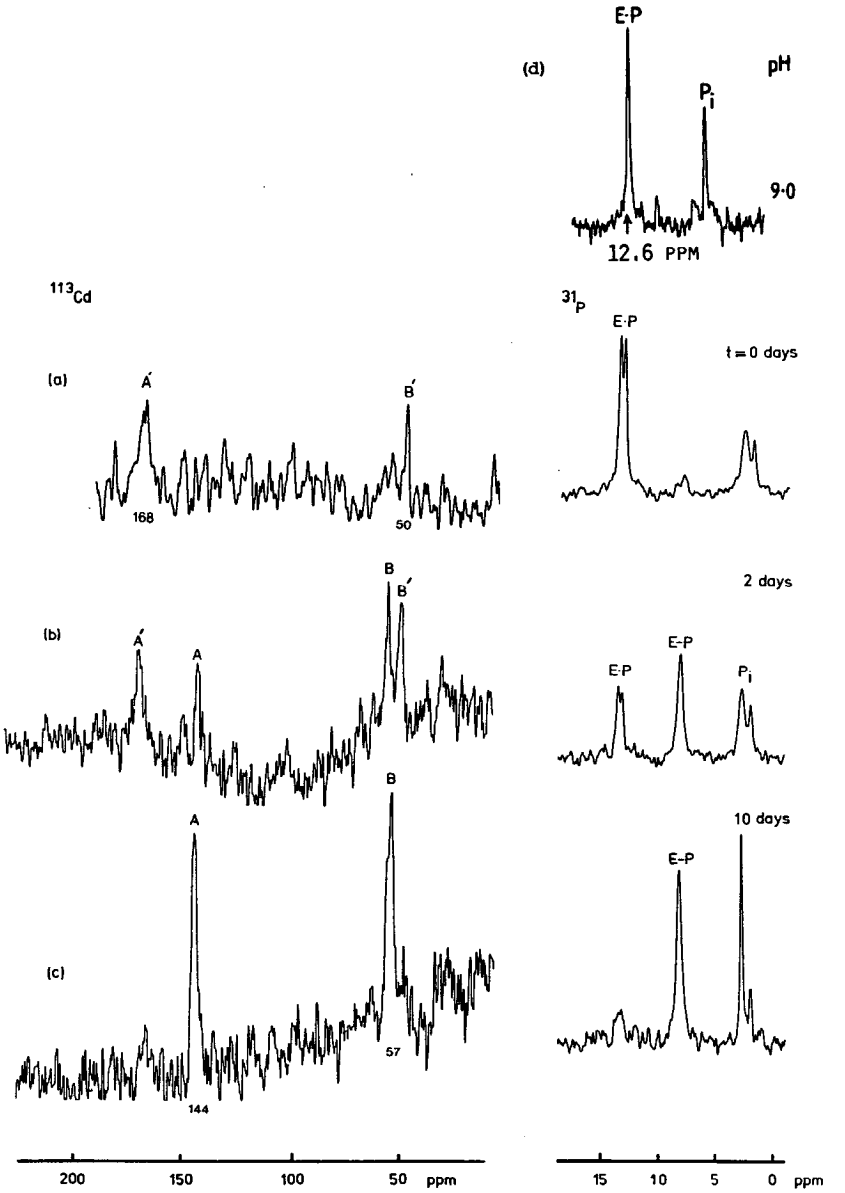

Figure 7 Time course of the slow phosphorylation of $(^{113}Cd_A{}^{113}Cd_{B\text{-}C})_2$AP (2.76 mM) containing two equivalents of P_i at pH 9.0. The spectra on the right are ^{31}P NMR (80.9 MHz) and on the left are ^{113}Cd NMR (*a*, 44.3 MHz; *b*,*c*, 19.96 MHz). (*d*) ^{31}P spectrum of the phospho-Zn(II)$_A$Cd(II)$_B$ alkaline phosphatase hybrid at pH 9.0. The data are from Ref. 32 and 36.

enzyme that has a ^{31}P chemical shift that moves upfield to 5.8 ppm from 8.7 ppm (Table 3).

The above NMR characterizations are graphically illustrated by both ^{113}Cd and ^{31}P NMR signals during the phosphorylation of ($^{113}Cd_A$ $^{113}Cd_{B-C})_2AP$ by inorganic phosphate. The E·P species (^{31}P doublet at 13 ppm) forms rapidly (Figure 7*a*). This species slowly phosphorylates the enzyme over a period of days (Figures 7*b*,*c*). At two days, half of the enzyme has become E-P (^{31}P singlet at 8.7 ppm). Simultaneously, the ^{113}Cd signals have each split into two, reflecting the different values for Cd_A and Cd_B in the E·P and E-P forms of the enzyme, respectively. Perhaps reflecting the release of the coordinate bond between the phosphate and $^{113}Cd_A$ in E·P, the shift of the ^{113}Cd signal from site A on formation of E-P is 20 ppm, while that from $^{113}Cd_B$ is only 8 ppm (Figure 7*b*). The metal-ion species at site A largely determines the pH at which [E·P] = [E-P] or the pH at which $k_3 = k_{-3}$ (21, 24, 33). This pH shifts from 5 for Zn_4AP to 8.7 for Cd_6AP, while remaining at pH 6 for the $(Zn_ACd_B)_2AP$ hybrid (Table 3). Because k_{-3} appears to be pH independent, based on the ^{18}O exchange out of $HP^{18}O_4^{2-}$ catalyzed by the enzyme, this extreme change in the pH dependence of k_3 must relate to an effect of Cd_A on the dephosphorylation of E-P.

Dephosphorylation of E-P is absolutely metal-ion dependent, and Cd is a "softer" metal than Zn and therefore is expected to affect lowering the pK_a of a coordinated water less. If the nucleophile required for the dephosphorylation of E-P were a metal-hydroxide formed from a solvent H_2O coordinated to Zn_A, then k_3 would vary with the $Zn\cdot OH_2 \rightleftharpoons Zn\cdot {}^{-}OH + H^+$ dissociation. The titration data in Figure 2 indicate that the pK_a of a water coordinated to Zn_A would have to be ~ 7.5 in order to match both the pH dependence of k_3 and the pH dependence of k_{cat}. Because below the pK_a of the $Zn\cdot OH_2$, the concentration of the $Zn\cdot {}^{-}OH$ nucleophile would continue to fall by 10-fold for each 1-unit further drop in pH, k_3 would fall as well. Thus, when the pH reaches a value where k_3 matches k_{-3}, E-P will build up along a sigmoid curve whose midpoint is the pH at which $k_3 = k_{-3}$ (Scheme 1). Because Cd_A moves the pH at which $k_3 = k_{-3}$ toward the alkaline by ~ 3.7 pH units, the postulate of a $metal_A$-hydroxide as the nucleophile in the dephosphorylation of Ser102 requires that the pK_a of the $Cd\cdot OH_2 \rightleftharpoons Cd\cdot {}^{-}OH + H^+$ equilibrium be at least 3.7 pH units higher than that for the corresponding zinc equilibrium. How much above pH 8.7 the pK_a of the $Cd\cdot OH_2$ is depends on the value of k_{-3}, which we do not know for the Cd enzyme.

The nucleophile in both the hydration and esterase reactions catalyzed by carbonic anhydrase is a Zn-hydroxide at the active center of the enzyme, and the $Zn\cdot OH_2 \rightleftharpoons Zn\cdot {}^{-}OH + H^+$ equilibrium is described by a pK_a of

6.8 (71). The substitution of Cd for the native Zn ion shifts this pK_a to 9.3, and the apparent pK_a of the sigmoid pH profile of k_{cat} for esterase activity shifts from 6.8 to 9.3 (71). Thus, a shift in the pK_a of a coordinated solvent molecule has a precedent in another zinc metalloenzyme and is one of the few changes expected of a Cd substitution that could account for such a dramatic shift in the pH dependence of a rate constant for an enzyme reaction.

CORRELATION OF STRUCTURE AND MECHANISM

Michaelis Complex with a Phosphate Monoester

The electron density map of the active center in the absence of phosphate indicates a bond between the oxygen of Ser102 and Zn2 (Figure 6*c*), supporting the notion that one of the functions of Zn2(A) is to activate the Ser hydroxyl to Ser-O^-. However, the 2-Å map of the E·P complex from which nucleophilic attack of the Ser O^- would occur shows that this coordination position is occupied by one of the phosphate oxygens, leaving the serine side chain free in the cavity (disordered). Nevertheless, some activation may be conferred by the positive charge density, and in the E·P complex, protons may not have access to the Ser-O^-. The structure of the E·P complex with the $(Zn_AZn_BMg_C)_2AP$ indicates that the four oxygens of the phosphate are each in contact with a positively charged center, one with Zn_A, two in a hydrogen bond network with the guanidino group of Arg166, and the fourth with Zn_B through the unusual P-O-Zn bond angle of almost 180° described earlier. Perhaps this unusual bond, rather than the lack of a bond, in the E·P complex of the cadmium enzyme accounts for the inability to observe detectable ^{113}Cd-^{31}P coupling to the ^{113}Cd at the B site.

The Zn1-O-P-O-Zn2 bridge and the two hydrogen bonds between the two other phosphate oxygens places the oxygen of Ser102 in the expected position for nucleophilic attack on the phosphorous nucleus, a position that would become one of the apical positions if a five-coordinate intermediate were formed. The oxygen coordinated to Zn1 would occupy the opposite apical position. These relationships are best seen in Figure 4*a*. If the E·P structure is extrapolated to that of E·ROP (with which E·P must share at least some features in common), then the oxygen coordinated to Zn_A must be the ester oxygen. None of the other positions would allow space for the attachment of an R group, which can range in size from CH_3 to a macromolecule. This observation suggests that in the normal hydrolysis reaction, Zn_A is an electrophile activating the leaving group, much as protonation of the ester oxygen does in the model systems. Thus, the alkaline phosphatase mechanism may have as significant a dissociative

component provided by activation of the leaving group by Zn_A as it does an associative component provided by the attack of Ser102, the latter activated by the second Zn ion. An electrophilic activation by the Zn would explain why the β values for k_{cat}/K_m observed for substrates that cannot protonate the leaving group (phosphopyridines) do not differ significantly compared with those that can (oxyesters) (51); both β values are equally small (51). A dissociative character of the alkaline phosphatase reaction has been suggested by the low magnitude of secondary isotope effects when the nonbridging oxygens of the substrate are labeled with ^{18}O (77). This is compatible with the observation that an alkoxide, RO^-, appears to be the species coordinated to $Zn_A(1)$ in the phosphotransferase mechanism (38). Thus a Zn_A-coordinated alkoxide as the immediate leaving group in normal hydrolysis is entirely possible.

The Phosphoseryl Intermediate

As noted above, the very large alkaline shift in the pH at which [E-P] = [E·P], induced by Cd at the A site (Table 3), provides a means for visualizing the E-P complex in the crystal structure. A normal-appearing ester bond has formed with Ser102 and the phosphate is slightly deeper in the active center cavity than in the case of the E·P complex (Figure 6*b*). The electron-density map of the E-P complex shows that Cd2 forms a coordinate bond with the ester oxygen of the seryl phosphate (Figure 6*b*). The latter would suggest that the metal in site B(2) has the same function in the second half of the mechanism as the metal in site A(1) has in the first half, i.e. activation of the leaving group. The possibility of a phosphate oxygen remaining in contact with Cd1 in the E-P complex is not clear from the electron-density map (Figure 6*b*). Mechanistic considerations suggest that if the nucleophile in the final hydrolysis reaction is a solvent coordinated to metal A(1), then the coordination of an electron-donating group of the substrate to the same metal ion as the nucleophile would not facilitate this step.

Hydrolysis of the Phosphoseryl Intermediate

The crystal structure of the E-P complex indicates that a solvent molecule in position to be a nucleophile adding to the phosphate nucleus from the apical position opposite to that occupied by the seryl ester would clearly be placed in the vicinity of Zn(1). An obvious choice is to place the solvent as one coordinated to Zn1 in the approximate position originally occupied by the coordinated phosphate ester oxygen in the E·P complex (Figure 4). For the reasons described in the previous section, the ionization of a coordinated solvent molecule on metal A is the simplest explanation for

the pH-rate profile and for the behavior of the pH-dependent E-P $\rightleftharpoons$ E·P equilibrium upon the Cd for Zn substitution.

Dissociation of the Product, Inorganic Phosphate, the Rate-Limiting Step

As discussed above, at alkaline pH (8 to 9) where alkaline phosphatase is maximally active, dissociation of the product, P_i, is rate limiting for the native $(Zn_AZn_BMg_C)_2$ enzyme, as most easily demonstrated by NMR methods. For the native enzyme, the reported values for k_4 (Scheme 1) have ranged from 20 to 50 s^{-1} (19, 44). This value is approximately the range reported in the literature for k_{cat}, 13–70 s^{-1}, under a variety of conditions (19, 29, 41, 63). At acid pH, the rate-limiting step changes to dephosphorylation of the phosphoseryl intermediate, primarily because of a dramatic fall in the rate constant, k_3, for this reaction from $\geqslant 300$ s^{-1} (pH 8) to ~ 0.5 s^{-1} (pH 5.5) (19). This fall in k_3 is compatible with the notion that the nucleophile for this dephosphorylation is a Zn-hydroxide at the A site that becomes protonated in the acid form of the enzyme, thus markedly reducing the concentration of active nucleophile present (21).

As outlined in the earlier section on kinetics, both the rate of phosphate dissociation, k_4, and the rate of phosphorylation of Ser102 by E·P, k_{-3}, depend on the species of metal ion present at both A and B sites. Both metal sites seem to be involved in the regulation of the phosphate dissociation because the rate for the Zn_ACd_B hybrid enzyme shows a less dramatic fall in k_4 to ~ 2 s^{-1}, compared with the Cd_ACd_B enzyme in which k_4 is < 1 s^{-1} (Table 2) (38). The structure of the E·P complex as revealed by the crystal structure does not directly suggest a reason for this metal-ion dependence of k_4. Because metal-phosphate bonds to both A- and B-site metal ions are required for phosphate binding, dissociation probably depends critically on the detailed charge distribution at the sites as well as on subtle aspects of the coordination geometry. The latter may be somewhat different for the larger Cd(II) ion, i.e. 0.97 Å compared with 0.74 Å for Zn(II). It is not clear, however, why the larger Cd(II) ion results in slower dissociation of phosphate.

Early kinetic studies called attention to the fact that an activation of alkaline phosphatase caused by increasing ionic strength should be distinguished from the "apparent" activation caused by the additive transferase activity (61). Because 1 M concentrations of Tris usually carry significant Cl^- concentrations as well, these separate effects can be confusing. The ionic strength effect (activation), e.g. from the addition of NaCl, can be accounted for by the fact that the anion, Cl^-, enhances the dissociation rate for phosphate as shown in Table 2. Even the relatively slow phosphate dissociation from the $(Zn_AMg_BMg_C)_2$AP can be enhanced $\sim$15-

fold by 1 M Cl^- (Table 2). The molecular mechanism of this effect appears adequately explained by the ^{35}Cl NMR (Zn_4Mg_2 enzyme) and ^{113}Cd NMR (Cd_6 enzyme) observations that Cl^- can occupy two coordination sites at the A-site metal ion (37). Thus, Cl^- is in competition with one of the phosphate-oxygen-metal bonds and can thus labilize the bound phosphate of E·P.

Because of the apparent lack of effect of pH on phosphate binding to the enzyme through the range of the second pK_a of phosphate, investigators have always argued that the phosphate is forced to bind to the enzyme active center as the dianion (63). The phosphate-dissociation rate is independent of pH from pH 8.8 to pH 5.5 as has been shown directly with ^{31}P NMR inversion transfer for Zn_4AP (38) (Figure 2). All forms of E-P show ^{31}P chemical shifts more downfield than the dianion of free phosphoserine, for which the $\delta = 4$ ppm (Table 3). The ^{31}P chemical shifts of all forms of E·P, with the exception of that for $(Zn_AMg_BMg_C)_2AP$, are downfield of that for the dianion forms of free P_i, $\delta = 3$ ppm. The $(Zn_AMg_BMg_C)_2AP$ enzyme has an unusually far upfield ^{31}P resonance for E·P (Table 3) and a very slow off rate for phosphate, $k_4 = 1.0$–$1.8\ s^{-1}$ (Table 2). This slowing of the rate-limiting step in the hydrolysis reaction is an adequate explanation for the fact that in the presence of an acceptor like Tris, where the majority of the reaction is phosphotransferase rather than hydrolysis, k_{cat} does not decrease for the $(Zn_AMg_BMg_C)_2AP$, while if no acceptor is present, k_{cat} is 10% of that for the native enzyme. This assertion follows because the dissociation of an ester, e.g. R′OP as the transferase product, is much faster than HOP as discussed in more detail below.

The Phosphotransferase Reaction

The transfer of the phosphate from E-P to an acceptor alcohol by alkaline phosphatase was discovered early in kinetic studies of the enzyme (26, 63). The fact that a two- to fourfold enhancement in the rate of RO^- release could be observed by adding an acceptor like Tris(tris-hydroxymethyl aminomethane) (Table 1) led to the routine inclusion of 1 M Tris in the standard assay of alkaline phosphatase. The enhanced rate of release of *p*-nitrophenolate made the assay significantly more sensitive. Product analysis showed that the enhanced activity resulted almost entirely from the formation of a new phosphate monoester, Tris-phosphate. The rate of formation of the original hydrolysis product, phosphate, remained relatively unaffected (63, 79).

Isolation of nonchromophoric phosphate esters is difficult, and relatively little quantitative data on the phosphotransferase reaction have accumulated over the years. Recently, ^{31}P NMR proved to be a convenient method

of simultaneously following the phosphotransferase and hydrolysis reactions (38). Most phosphate monoesters, even those with relatively similar R groups, have sufficiently different ^{31}P chemical shifts to be distinguished. The separate signals for *p*-nitrophenylphosphate, P_i, and phospho-Tris are shown in Figure 8*a* illustrating a ^{31}P NMR spectrum of a standard assay mix (20 mM *p*-nitrophenylphosphate-1 M Tris) a few minutes after adding assay concentrations of alkaline phosphatase.

Figure 8*b* shows examples of the pH-dependencies of phosphotransferase reactions as followed by ^{31}P NMR, employing two rather different acceptors, Tris and glycerol. The data are presented as the ratio of new ester product to the hydrolysis product, phosphate, as a function of time, which is also the ratio of the rates of the two separate reactions,

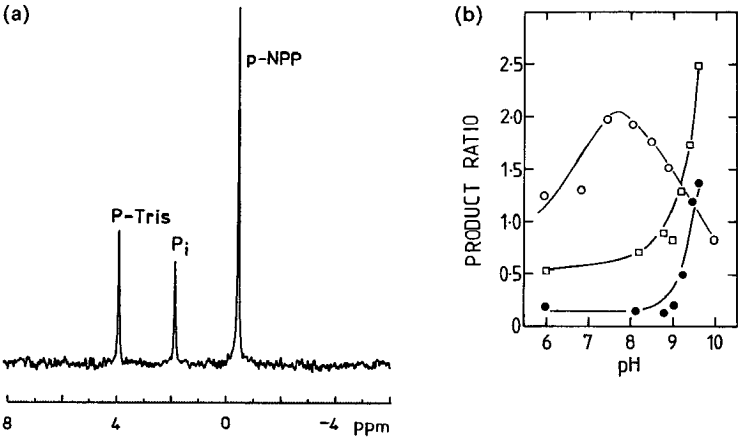

Figure 8 (*a*) ^{31}P NMR (80.9 MHz) spectra of substrate, *p*-nitrophenyl phosphate and products, inorganic phosphate, and O-Tris phosphate during hydrolysis and phosphotransfer as catalyzed by alkaline phosphatase. The composition at the start of reaction was 20 mM *p*-nitrophenyl phosphate in 1 M Tris or 3 M glycerol, pH 8, 293 K. To this was added alkaline phosphatase (5×10^{-8} M). The spectra were collected after about 50% hydrolysis and represent 80 scans. (*b*) pH Dependence of transferase and hydrolase products in the presence of 1 M Tris and 3 M glycerol. (*Open circle*) Ratio of initial rates of formation of Tris phosphate to inorganic phosphate; (*open square*) ratio of initial rates of formation of glycerol C1, C3, and C2 monophosphate to inorganic phosphate; (*solid circle*) ratio of initial rates of formation of glycerol C2 monophosphate to glycerol C1,C3 monophosphate. Note that at pH 9.5 the C2 transferase product exceeds the C1+C3 product by the ratio 1.3 : 1.0. The reaction mixture in the case of glycerol contained initially 3 M glycerol in 50 mM Tris (the latter solely as buffer and not at high enough concentration to result in competition with 3 M glycerol). Enzyme (10^{-7}–10^{-8} M) was used depending on pH. The substrate concentration was 20 mM. The figure is reproduced from Ref. 38.

phosphotransferase/phosphohydrolyase. The two curves for glycerol represent the formation of the equivalent C1 + C3 monophosphates and the C2 monophosphate. All three hydroxyl groups of glycerol are approximately equally phosphorylated by the enzyme. Tris is a much more effective acceptor in the neutral pH range than glycerol. The phosphotransferase reaction also increases in rate as the pH approaches the pK_a of the amino group, ~8 for Tris (63). This observation led to the suggestion that the neutral species of the amino alcohols were the most effective acceptors (63). The transferase activity of Tris, however, peaks at pH 8, falling rapidly to higher pH values (Figure 8*b*). At pH 9 and above, nonamino alcohols like glycerol, ethanol, and propanol are substantially more efficient acceptors than Tris (Figure 8*b*).

The rapid increase in the phosphate transfer to aliphatic alcohols above pH 9 is compatible with an arrangement in which the accepting alcohol is in the alcoxide form when bound at the active center and accepts the phosphoryl group from the seryl phosphate intermediate (38). If the oxygen of the acceptor coordinates Zn_A, as seems likely (38), then the apparent pK_a of the -C-OH will be lowered. An alcoxide has also been postulated to be the form of ethanol bound to alcohol dehydrogenase (82), another zinc enzyme in which an open coordination position on a zinc ion is the driving force for the formation of the alcoxide below its pK_a. At concentrations 0.5 M or greater, Tris and glycerol shift the ^{113}Cd resonance from the A site upfield by 14 and 6 ppm, respectively, at pH 9 (38). These ^{113}Cd chemical shift changes may represent the displacement of a water ligand by the alcoxide of the acceptor (38). Both the enhanced acceptor efficiency of the amino alcohols below the pK_a of the amino group and the rapid decline upon deprotonation of the amino group (Figure 8*b*) could result from the lowering of the pK_a of the $-CH_2-OH$ group caused by the adjacent $-C-NH_3^+$ group such that the alcoxide of the amino alcohols is formed more readily (has a lower pK_a) below the pK_a of the amino group than when the neutral form of the amino group is present.

SUMMARY OF THE MECHANISM OF ALKALINE PHOSPHATASE AS BASED ON SOLUTION DATA AND THE CRYSTAL STRUCTURE

Figure 9 shows the Michaelis complex of the dianion of a phosphate monoester bound to the active center of Ser102 along with the steps leading to the phosphorylation of Ser102 and its subsequent dephosphorylation. The probable structural relationships are taken from the crystal structure of the E·P complex of the native zinc enzyme (Figure 4*b*) and the E-P complex of the cadmium enzyme (Figure 6*b*). Zn_A coordinates the ester

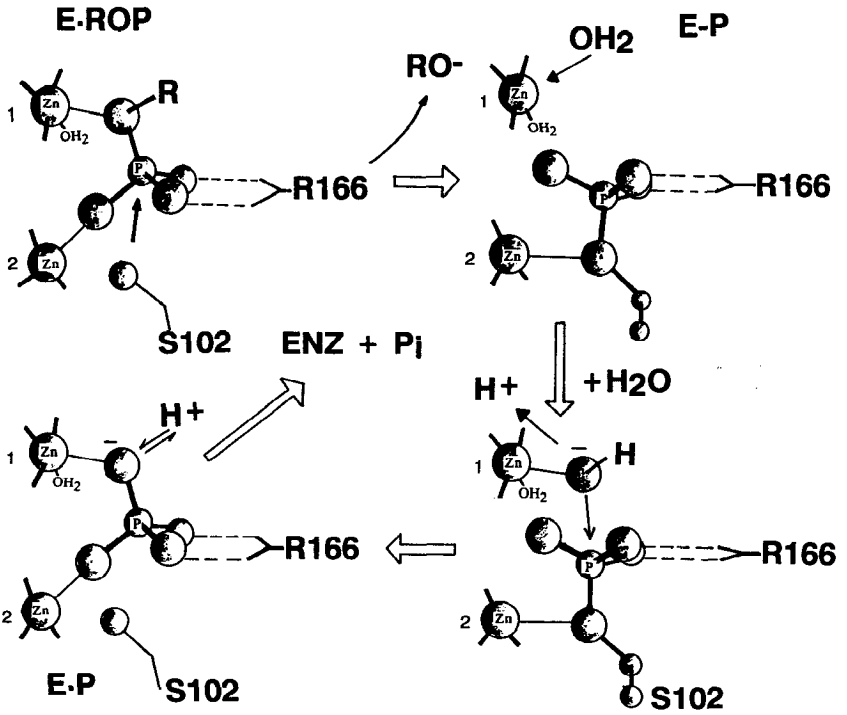

Figure 9 Major intermediates in the proposed mechanism of action of alkaline phosphatase. The dianion of a phosphate monoester, $ROPO_4^{2-}$, forms E·ROP in which the ester oxygen coordinates Zn1; a second oxygen coordinates Zn2, forming a phosphate bridge between the Zn1 and Zn2; while the other two phosphate oxygens form hydrogen bonds (*dashed lines*) with the guanidium group of R166. Ser102 is the nucleophile in the first half of the reaction and would occupy the position opposite to the leaving group, RO^-, in a five-coordinate intermediate. Upon formation of E-P, the phosphate (as the dianion of a phosphoseryl residue) moves slightly into the cavity of the active center, but maintains a coordinate bond between Zn2 and the ester oxygen as well as the two hydrogen bonds with R166. A water molecule coordinates Zn1 in the position occupied originally by the ester oxygen of the substrate. At alkaline pH, the water dissociates a proton to become Zn-$^-$OH in position to be the nucleophile for the hydrolysis of the phosphoseryl ester. E·P forms as the phosphate moves away from the serine and as one of the phosphate oxygens again coordinates Zn1 to reestablish a phosphate bridge. E·P is pictured as a phosphate trianion for the reasons discussed in the text. Dissociation of phosphate from E·P is the slowest, 35 s^{-1}, and therefore the rate-limiting, step.

oxygen, activating the leaving group. Zn_B, 3.9 Å away, coordinates a second phosphate oxygen, while the other two phosphate oxygens form hydrogen bonds with the guanidino group of Arg166. The leaving group is pictured as the alcoxide, RO^-. Activation of this leaving group by the

A-site metal ion via a bond with the ester oxygen appears to be one of the functions of this ion in the first stage of the alkaline phosphatase reaction. The oxygen of Ser102 is in the other apical position to form the new ester bond with the phosphorous. Dissociation of RO^- and formation of the phosphoseryl intermediate is associated with movement of the phosphate farther into the cavity (Figure 6*b*). Hence, when the alcoxide leaves, its coordination site on Zn_A can be occupied by a water molecule that must dissociate a proton and become a Zn-$^-$OH. The strongest evidence for this metal-induced proton dissociation is the large alkaline shift (3.7 pH units) in the pH dependence of the $E \cdot P \rightleftharpoons E\text{-}P$ equilibrium when the much softer metal ion, Cd(II), is substituted for Zn(II). The Zn-$^-$OH, placed in the apical postion opposite to the seryl ester, occupies the place of the original leaving group and thus is ideally positioned to be the nucleophile in the second stage of the hydrolysis reaction (Figure 9).

The second stage of the reaction is nearly a mirror image of the first stage. Zn_B now activates the leaving group by forming a coordinate bond with the ester oxygen of the phosphoseryl residue (Figure 9). The hydroxyl coordinated to Zn_A attacks the phosphorous from the other apical position, and the transition state will decay into $E \cdot P$. The issue of whether the new phosphate oxygen remains negatively charged is discussed below, but the dissociation of phosphate anion in the $E \cdot P$ intermediate is remarkably slow, 35 s^{-1}.

As discussed in connection with the phosphotransferase reaction, why the dissociation of $R_2OPO_3^{2-}$ is more rapid than that of $HOPO_3^{2-}$ if the latter is bound as the dianion is unclear. One possibility is that coordination of phosphate to both Zn ions as well as hydrogen bonding of the other two oxygens to the guanidino group of Arg166 forces the formation of the trianion, OPO_3^{3-}. On the other hand, the bound $ROPO_3^{2-}$ can only be a dianion. Zn_A does seem to be capable of lowering the pK_a of bound water by several pH units as well as inducing the alcoxide in the phosphotransferase reaction. Thus, lowering the third pK_a of phosphate may not be so unexpected as it might at first appear. Such a postulate would provide an explanation as to why dissociation of phosphate from the active center is so much slower than that for the dianion of a phosphate ester. The higher negative-charge density would also explain why phosphorylation of Ser102 by both phosphate and thiophosphate is so slow compared to phosphorylation by any phosphate ester. The pK_a of the leaving group for thiophosphate, H_2S, is 6.9 compared to a pK_a of 15.7 for HOH, the leaving group in phosphorylation from phosphate. Yet in the presence of rate-controlling phosphorylation, the difference in the phosphorylation of Ser102 by these two agents is at most only twofold (Table 1), despite the large ΔpK_a between the leaving groups. If both substrates were bound as

trianions, poor leaving groups (probably requiring protonation first) and high charge density around the phosphorous could account for the very slow phosphorylation step as well as slow dissociation of the noncovalently bound species.

In the case of most enzyme-catalyzed phosphorylation or phosphotransferase reactions, investigators have tended to assume that such biological reactions were nucleophilic and associative and formed classic five-coordinate intermediates, the leaving group departing from the opposite apical position. This assumption was made despite the fact that in model systems most phosphate mono- and diester hydrolyses apparently proceed by a dissociative mechanism with the transient production of the highly electrophilic metaphosphate, [PO_3^-] (6, 49, 78). Only phosphate triester hydrolysis follows a nucleophilic path in model systems (6, 49, 78). Enzymes could presumably make the nucleophilic path more favorable by creating protein-binding sites that successfully reduced the negative charge around phosphate, a significant inhibitory factor in mono- and diester hydrolysis in model systems. Determination of the predicted chirality changes around phosphate during enzyme-catalyzed phosphate incorporations, i.e. inversion if no covalent enzyme intermediate was formed and retention if a covalent enzyme intermediate was formed as in alkaline phosphatase, tended to solidify the nucleophilic point of view. However, the finding that the Zn ions activate the leaving group in both the initial phosphorylation of the active-center serine and its dephosphorylation suggests that there may be significant dissociative character to both reactions. While the enzyme might hold a metaphosphate rigid enough to prevent scrambling of chirality, the evidence that the phosphate oxygens exchange positions relatively rapidly in the Co(II) enzyme does not favor the existence of free PO_3^- at the active site. Whether a classic five-coordinate intermediate is a true transition state in the alkaline phosphatase reaction remains an open question.

SITE-DIRECTED MUTANTS OF *E. COLI* ALKALINE PHOSPHATASE

Cloning of the *phoA* gene has allowed researchers to employ site-directed mutagenesis to change several of the amino acid side chains at the active center of alkaline phosphatase. The results of mutations at Ser102 and Arg166 have been most informative relative to mechanism, while mutations of several surrounding residues have revealed subtle influences on the rate. The results of these mutations are summarized below.

Ser102 → Cys102, Ala102, Leu102

The Ser102 → Cys102 mutant shows between 30 and 90% of normal activity against *p*-nitrophenyl phosphate and 2,4-dinitrophenyl phosphate depending on conditions. The range of turnover values results both from the fact that the phosphotransferase/phosphohydrolase ratio is increased and that k_{cat} depends on the nature of the leaving group. The Cys102 enzyme has a k_{cat} of 4.6 s^{-1} with 4-nitrophenyl phosphate and a k_{cat} of 15 s^{-1} with 2,4-dinitrophenyl phosphate under conditions where k_{cat} for the wild-type enzyme is 18 s^{-1} (39). In addition, the pH profile of the Cys102 enzyme shows no clearly apparent pK_a of activity. Lastly, a covalent S-phosphorothioate cannot be isolated from the enzyme by quenching at low pH (39). Most of the above findings on the Cys102 mutant can be explained if the rate-limiting step has changed to phosphorylation throughout the pH range. Throughout the pH range, phosphorylation of the native enzyme by $ROPO_4^{2-}$ occurs at the rate of 10^2 to 10^3 s^{-1}; thus, the phosphorylation rate can fall by 10- or even 100-fold without significantly lowering k_{cat}. These findings also suggest that dephosphorylation of the S-phosphorothioate formed with Cys102 is occuring more rapidly than for the normal covalent intermediate. A detailed kinetic study is required to sort out the rate constants of the Cys102 mutant. Phosphotransfer from a ^{16}O-, ^{17}O-, and ^{18}O-labeled phosphate ester to an acceptor catalyzed by the Cys102 mutant revealed retention of configuration around the phosphorous, proving that the reaction pathway has not been substantially changed (12).

The Ser102 → Ala102 or Leu102 mutants are not completely devoid of activity. The k_{cat} values are reported to be ~1/1000 and ~1/500 of those for the wild-type enzyme (14). K_m values for $ROPO_4^{2-}$ and K_i values for P_i are reported to be normal as is the pH-rate profile. Because residue 102 is not directly involved in the structure of E·P, the lack of alteration in substrate and phosphate binding is not surprising. Since Zn_A carries two coordinated H_2O molecules, as shown using NMR relaxation methods (37, 64), a water remaining on Zn_A may be in a position to directly attack the ester of E·ROP at a low rate. An alcoxide, R_2O^-, could do the same and account for the detection of some phospho-Tris formed by these mutants (14).

Arg166 → Lys166, Glu166, Ser166, Ala166

All four mutations of Arg166 result in enzymes that remain active but demonstrate an increase in K_m and a decrease in phosphate affinity (13, 15). Although a decrease in phosphate binding affinity might increase the

rate of phosphate dissociation, k_4, and therefore k_{cat}, the fact that the opposite occurs suggests that the loss of a positively charged center, helping to reduce the negative charge density at phosphorous, is the more important function. This fact also suggests that despite a significant dissociative aspect to the mechanism, the alkaline phosphatase reaction must retain significant aspects of a nucleophilic hydrolysis mechanism. This conclusion is supported by the finding for these mutants that when the nucleophile is water (hydrolysis), a relatively poor nucleophile, k_{cat} is reduced more by the mutation than when RO^- (phosphotransfer), a better nucleophile, is the nucleophile in the second half of the reaction. Likewise, the leaving group in the first half of the mechanism, phosphorylation of Ser102, has a more pronounced effect on the observed k_{cat} of the Arg166 mutants, e.g. k_{cat} decreases 10-fold on shifting from *p*-nitrophenolate as the leaving group to phenolate for both the Lys and Glu mutants. The effect of the Lys mutant must result from the different topological placement of the positive charge by the shorter lysyl side chain.

The fact that changes related to the bond-making and -breaking steps are now reflected in k_{cat} suggest that these mutations may have changed the relative values of the rate constants such that phosphate departure is no longer the slowest and therefore exclusively rate-limiting step. Further investigation is needed. While reduced in affinity, the phosphate binding is nevertheless adequately maintained in the Arg166 mutants by the interactions with the metal ions and the further hydrogen bonds with bridging water molecules to Mg_C and Lys328 (Figure 4*b*). E. E. Kim & H. W. Wyckoff (in preparation) have determined the crystal structure of the Arg166 → Ala166 mutant, which shows no changes in the active center except for the truncation of the density at the β-carbon of residue 166. Thus, the changes in the reaction parameters described above can be attributed exclusively to the functions of the Arg166 side chain.

Lys328 → His328, Ala328

Despite the conservation of many of the active-site residues found at the active center of the *E. coli* enzyme in several mammalian alkaline phosphatase isozymes, it has been puzzling why the mammalian enzymes uniformly show k_{cat} values at least an order of magnitude larger than that of the bacterial enzyme (for review, see 22). One intriguing structural finding at the active center of the bacterial enzyme is that Lys328, replaced by a His in all mammalian alkaline phosphatases, is bridged to the bound phosphate in E·P through a water molecule (Figure 4*b*). The latter water molecule is also hydrogen bonded to one carboxyl oxygen of Asp327, the bidentate ligand to Zn_A. The other oxygen of Asp327 makes a hydrogen bond with the N3 of His372 as discussed in the section on structure.

Because of the difference in the nature of residue 328 between the mammalian and bacterial enzymes and the close association of the Lys328 side chain with the A-site metal ligands as well as with phosphate via hydrogen bonds, two single site mutations of this residue have been examined, Lys328 → His328 and Lys328 → Ala328 (54, 81).

At pH 10.3, the Lys328 → Ala328 mutant shows a 14-fold increase in k_{cat} in the presence of Tris as an acceptor and a 6-fold increase in k_{cat} in the absence of the acceptor (15). At pH 8.0 in 1 M Tris, k_{cat} for the mutant enzyme was 81 s^{-1} and for the wild-type enzyme was 16 s^{-1}. The Lys328 → His328 is similar, but the enhancement of k_{cat} is not as large. Both mutant enzymes show reduced affinity for phosphate. K_m for $ROPO_4^{2-}$ is increased from 21 μM for the wild-type enzyme to 159 μM for the Ala328 mutant and 58 μM for the His328 mutant. Some significant changes are observed in the alkaline pH-rate profile of the mutant enzymes both in the presence and absence of a phosphate acceptor as well as in the magnitude and rate of the burst observed at both acid and alkaline pH, suggesting that the relative values of k_3 (dephosphorylation of E-P) and k_4 (phosphate dissociation) may have been changed by the mutation. Xu & Kantrowitz (81) suggest these changes might result from a change in the pH dependence of k_3, reflecting a change in the pK_a of the solvent H_2O coordinated to Zn_A. We lack sufficient detail on the pH dependence of the individual rate constants to be certain of the precise origin of the observed changes in pH-dependent functions. In another zinc enzyme, carbonic anhydrase, a series of detailed studies of rate-constant changes vs pH for several site mutations and a crystal structure of an isozyme carrying three of the side-chain changes show that changes in residues near the active center that alter the hydrogen-bonding patterns of the ordered water molecules near the Zn-coordinated solvent are far more effective in altering the pK_a of the coordinated solvent than are mutations of charged residues in the active site cavity that do not alter the hydrogen bond structure (73).

Several other site mutations of residues near the active center increase k_{cat}. These include Asp101 → Ala101, which increases k_{cat} 4.2-fold (80), as well as several mutations in the polypeptide chain region from residue 99 to 109. Mandecki et al (54) screened for "up" mutants in this region and found that V99A, T100V, A103D, A103C, and T107V all increase k_{cat} two- to fourfold. Residues 101 to 112 form a helical stem that holds Ser102 in place at the active center. Thus, alterations in k_{cat} are not surprising. What is perhaps unexpected is that most changes enhance k_{cat}. The assays are in 50 mM Tris; thus, the increases in k_{cat} primarily relate to the hydrolysis reaction. In the case of the *E. coli* enzyme, in which the dissociation of the phosphate is a very slow and rate-limiting step at alkaline pH, several slight perturbations of the topology at the active center can enhance

this step. What evolutionary advantage prevented such mutations from evolving naturally is unclear. Perhaps phosphotransferase (not inhibited by phosphate departure) is a much more important reaction to *E. coli* than we currently appreciate because the natural acceptor has not been identified.

SUMMARY

Alkaline phosphatase was the first zinc enzyme to be discovered in which three closely spaced metal ions (two Zn ions and one Mg ion) are present at the active center. Zn ions at all three sites also produce a maximally active enzyme. These metal ions have center-to-center distances of 3.9 Å (Zn1-Zn2), 4.9 Å (Zn2-Mg3), and 7.1 Å (Zn1-Mg3). Despite the close packing of these metal centers, only one bridging ligand, the carboxyl of Asp51, bridges Zn2 and Mg3. A crystal structure at 2.0-Å resolution of the noncovalent phosphate complex, E·P, formed with the active center shows that two phosphate oxygens form a phosphate bridge between Zn1 and Zn2, while the two other phosphate oxygens form hydrogen bonds with the guanidium group of Arg166. This places Ser102, the residue known to be phosphorylated during phosphate hydrolysis, in the required apical position to initiate a nucleophilic attack on the phosphorous. Extrapolation of the E·P structure to the enzyme-substrate complex, $E \cdot ROPO_4^{2-}$, leads to the conclusion that Zn1 must coordinate the ester oxygen, thus activating the leaving group in the phosphorylation of Ser102. Likewise, Zn2 appears to coordinate the ester oxygen of the seryl phosphate and activate the leaving group during the hydrolysis of the phosphoseryl intermediate. Both of these findings suggest that there may be a significant dissociative character to each of the two displacements at phosphorous catalyzed by alkaline phosphatase. A water molecule (or hydroxide) coordinated to Zn1 following formation of the phosphoseryl intermediate appears to be the nucleophile in the second step of the mechanism. Dissociation of the product phosphate from the E·P intermediate is the slowest, 35 s^{-1}, and therefore the rate-limiting, step of the mechanism at alkaline pH.

Since the determination of the initial crystal structure of alkaline phosphatase, two other crystal structures of enzymes involved in phosphate ester hydrolysis have been completed that show a triad of closely spaced zinc ions present at their active centers. These enzymes are phospholipase C from *Bacillus cereus* (structure at 1.5-Å resolution) (43) and P1 nuclease from *Penicillium citrinum* (structure at 2.8-Å resolution) (74). Both enzymes hydrolyze phosphodiesters. Substrates for phospholipase C are phosphatidylinositol and phosphatidylcholine, while P1 nuclease is an

endonuclease hydrolyzing single stranded ribo- and deoxyribonucleotides. P1 nuclease also has activity as a phosphomonoesterase against 3′-terminal phosphates of nucleotides. The Zn ions in both enzymes form almost identical trinuclear sites. Zn1 and Zn3 are ~3.2 Å apart and are linked by a bridging carboxylate of an Asp residue as well as a bridging H_2O or ^-OH ion. Zn2 is an isolated site ~5.8 Å from Zn1 and ~4.7 Å from Zn3.

Are the three enzymes with trinuclear Zn sites at their active centers related? The general arrangement of the zinc ions is similar, but alkaline phosphatase and the other two enzymes are significantly different. All three metal sites in P1 nuclease and phospholipase C are typical Zn binding sites with mixed oxygen and nitrogen donors, while the third site in alkaline phosphatase is made up of all oxygen donors, which may explain its preference for Mg. The aspartate carboxylate bridging two of the Zn ions appears to define a binuclear zinc site in the two diesterases. In contrast, the bridging aspartate carboxylate defines the Zn-Mg pair in native alkaline phosphatase. As discussed in this review, the two nonbridged Zn ions, 3.9 Å apart in alkaline phosphatase, appear to form the major functional pair forming the phosphate bridge. In contrast, the few substrate analog binding studies done on the diesterases suggest that the isolated Zn2 site interacts with the phosphate diester (43). On the other hand, difference maps for phosphate bound to both P1 nuclease and phospholipase C show that an interaction with inorganic phosphate can take place involving coordination to all three zinc ions and raises the possibility that all three Zn ions could be catalytically involved at some stage of a complete mechanism.

Alkaline phosphatase is not closely related structurally to the other two enzymes. Alkaline phosphatase has a relatively small amount of α-helical structure on both faces of a large core of parallel and antiparallel β-sheets. The secondary structure of the two diesterases is composed almost entirely of α-helices, and their structures are closely related (43, 74). In addition, alkaline phosphatase forms a phosphoseryl intermediate, while both P1 nuclease and phospholipase C catalyze single-step hydrolyses, inverting the chirality around phosphate. While it is too early to state whether the trinuclear zinc sites found in the three phosphohydrolases reflect related functions, the data available at present suggest that the presence of multiple Zn ions located at a single enzyme active center add many alternatives to the reaction pathways available to zinc metalloenzymes.

ACKNOWLEDGMENT

I thank Harold W. Wyckoff and Eunice Kim for many helpful discussions and suggestions. The crystallography of alkaline phosphatase was supported by Grant GM22778. Original work in the author's laboratory was supported by NIH Grant DK09070.

Literature Cited

1. Anderson, R. A., Bosron, W. F., Kennedy, F. S., Vallee, B. L. 1975. *Proc. Natl. Acad. Sci. USA* 72: 2989–93
2. Applebury, M. L., Coleman, J. E. 1969. *J. Biol. Chem.* 244: 709–18
3. Applebury, M. L., Johnson, B. P., Coleman, J. E. 1970. *J. Biol. Chem.* 245: 4968–76
4. Bachman, B. J., Low, K. B., Taylor, A. L. 1976. *Bacteriol. Rev.* 40: 116–67
5. Bale, J. R. 1978. *Fed. Proc.* 37: 1287
6. Benkovic, S. J., Schray, K. J. 1973. *Enzymes* 8: 201–38
7. Benson, S. A., Hall, M. N., Silhavy, T. J. 1985. *Biochemistry* 54: 101–34

7a. Bertini, I., Luchinat, C., Maret, W., Zeppezaur, M., eds. 1986. *Zinc Enzymes.* Basel: Birkhäuser

8. Bloch, W. A., Schlessinger, M. J. 1973. *J. Biol. Chem.* 248: 5794–5805
9. Bock, J. L., Cohn, M. 1978. *J. Biol. Chem.* 253: 4082–85
10. Bosron, W. F., Anderson, R. A., Falk, M. C., Kennedy, F. S., Vallee, B. L. 1977. *Biochemistry* 16: 610–14
11. Bradshaw, R. A., Cancedda, F., Ericsson, L. H., Neuman, P. A., Piccoli, S. P., et al. 1981. *Proc. Natl. Acad. Sci. USA* 78: 3473–77
12. Butler-Ransohoff, J. E., Kendall, D. A., Freeman, S., Knowles, J. R., Kaiser, E. T. 1988. *Biochemistry* 27: 4777–80
13. Butler-Ransohoff, J. E., Kendall, D. A., Kaiser, E. T. 1988. *Proc. Natl. Acad. Sci. USA* 85: 4276–78
14. Butler-Ransohoff, J. E., Rokita, S. E., Kendall, D. A., Banzon, J. A., Carano, K. S., Kaiser, E. T., Matlin, A. R. 1992. *J. Org. Chem.* 57: 142–45
15. Chaidaroglou, A., Brezinski, J. D., Middleton, S. A., Kantrowitz, E. R. 1988. *Biochemistry* 27: 8338–43
16. Chaidaroglou, A., Kantrowitz, E. R. 1989. *Protein Eng.* 3: 127–32
17. Chang, C. N., Inouye, H., Model, P., Beckwith, J. 1980. *J. Bacteriol.* 142: 726
18. Chlebowski, J. F., Armitage, I. M., Tusa, P. P., Coleman, J. E. 1976. *J. Biol. Chem.* 251: 1207–16
19. Chlebowski, J. F., Coleman, J. E. 1974. *J. Biol. Chem.* 249: 7192–7202
20. Chlebowski, J. F., Coleman, J. E. 1976. *J. Biol. Chem.* 251: 1202–6
21. Coleman, J. E. 1987. In *Phosphate Metabolism and Cellular Regulation in Microorganisms*, ed. A. Torriani-Gorini, F. G. Rothman, S. Silver, A. Wright, E. Yagil, pp. 127–38. Washington, DC: Am. Soc. Microbiol.
22. Coleman, J. E., Besman, M. J. A. 1987. In *Hydrolytic Enzymes*, ed. A. Neuberger, K. Brocklehurst, pp. 377–406. New York: Elsevier
23. Coleman, J. E., Chlebowski, J. F. 1979. *Adv. Inorg. Biochem.* 1: 1–66
24. Coleman, J. E., Gettins, P. 1986. See Ref. 7a, pp. 77–99
25. Coleman, J. E., Nakamura, K., Chlebowski, J. F. 1983. *J. Biol. Chem.* 258: 386–95
26. Dayan, J., Wilson, I. B. 1964. *Biochim. Biophys. Acta* 81: 620–28
27. Engström, L. 1961. *Biochim. Biophys. Acta* 52: 49–59
28. Engström, L., Agren, G. 1962. *Biochim. Biophys. Acta* 56: 606–7
29. Fernley, H. N., Walker, P. G. 1969. *Biochem. J.* 111: 187–94
30. Fossett, M., Chappelet-Tordo, D., Lazdunski, M. 1974. *Biochemistry* 13: 1783–88
31. Garen, A., Levinthal, C. 1960. *Biochim. Biophys. Acta* 38: 470–83
32. Gettins, P., Coleman, J. E. 1983. *J. Biol. Chem.* 258: 396–407
33. Gettins, P., Coleman, J. E. 1983. *J. Biol. Chem.* 258: 408–16
34. Gettins, P., Coleman, J. E. 1983. *Adv. Enzymol.* 55: 381–452
35. Gettins, P., Coleman, J. E. 1982. *Fed. Proc.* 41: 2966–73
36. Gettins, P., Coleman, J. E. 1984. *J. Biol. Chem.* 259: 4991–97
37. Gettins, P., Coleman, J. E. 1984. *J. Biol. Chem.* 259: 11036–40
38. Gettins, P., Metzler, M., Coleman, J. E. 1985. *J. Biol. Chem.* 260: 2875–83
39. Ghosh, S. S., Back, S. C., Rokita, S. E., Kaiser, E. T. 1986. *Science* 231: 145–48
40. Grosser, P., Husler, J. 1912. *Biochem. Z.* 39: 1
41. Halford, S. E., Bennett, N. G., Trentham, D. R., Gutfreund, H. 1969. *Biochem. J.* 114: 243–51
42. Horiuchi, T., Horiuchi, S., Mizuno, D. 1959. *Nature (London)* 183: 1529–30
43. Hough, E., Hansen, L. K., Birknes, B., Jynge, K., Hansen, S., et al. 1989. *Nature (London)* 338: 357–60
44. Hull, W. E., Halford, S. E., Gutfreund, H., Sykes, B. D. 1976. *Biochemistry* 15: 1547–61
45. Inouye, H., Barnes, W., Beckwith, J. 1982. *J. Bacteriol.* 149: 434–39
46. Jones, S. R., Kindman, L. A., Knowles, J. R. 1978. *Nature (London)* 257: 564–65
47. Kim, E. E., Wyckoff, H. W. 1989. *Clin. Chim. Acta* 186: 175–88
48. Kim, E. E., Wyckoff, H. W. 1991. *J. Mol. Biol.* 218: 449–64

49. Knowles, J. R. 1980. *Annu. Rev. Biochem.* 49: 877–919
50. Krishnaswamy, M., Kenkare, U. W. 1970. *J. Biol. Chem.* 245: 3956–63
51. Labow, B. I. 1989. *Mechanisms of phosphoryl transfer by alkaline phosphatase from* E. coli. MS thesis. Brandeis Univ.
52. Levine, D., Reid, T. W., Wilson, I. B. 1969. *Biochemistry* 8: 2374–80
53. Ludke, D., Bernstein, J., Hamilton, C., Torriani, A. 1984. *J. Bacteriol.* 159: 19–25
54. Mandecki, W., Shallcross, M. A., Sowadski, J., Tomazic-Allen, S. 1991. *Protein Eng.* 4: 801–4
55. McComb, R. B., Bowers, G. N., Posen, S. 1979. *Alkaline Phosphatase.* New York: Plenum
56. Michaelis, A., Beckwith, J. 1982. *Annu. Rev. Microbiol.* 36: 435–65
57. Muller, M., Blobel, G. 1984. *Proc. Natl. Acad. Sci. USA* 81: 7737–41
58. Mushak, P., Coleman, J. E. 1972. *Biochemistry* 11: 201–5
59. Neumann, H. 1968. *J. Biol. Chem.* 243: 4671–76
60. Petitclerc, C., Lazdunski, C., Chappelet, D., Moulin, A., Lazdunski, M. 1970. *Eur. J. Biochem.* 14: 301–8
61. Plocke, D. J., Vallee, B. L. 1962. *Biochemistry* 1: 1039–43
62. Plocke, D. J., Levinthal, C., Vallee, B. L. 1962. *Biochemistry* 1: 373–78
63. Ried, T. W., Wilson, I. B. 1971. *Enzymes* 4: 373–415
64. Schulz, C., Bertini, I., Viezzoli, M. S., Brown, R. D., Koenig, S. H., Coleman, J. E. 1989. *Inorganic Chem.* 28: 1490–96
65. Schwartz, J. H. 1963. *Proc. Natl. Acad. Sci. USA* 49: 871–78
66. Schwartz, J. H., Lipmann, F. 1961. *Proc. Natl. Acad. Sci. USA* 47: 1996–2005
67. Schwartz, J. H., Crestfield, A. M., Lipmann, F. 1963. *Proc. Natl. Acad. Sci. USA* 49: 722–29
68. Sowadski, J. M., Handschumacher, M. D., Murthy, H. M. K., Foster, B. A., Wyckoff, H. W. 1985. *J. Mol. Biol.* 186: 417–33
69. Stein, S. S., Koshland, D. E. 1952. *Arch. Biochem. Biophys.* 39: 229–30
70. Suzuki, U., Yoshimura, K., Takaishi, M. 1907. *Bull. Coll. Argric. Tok. Imp. Univ.* 7: 503
71. Tashian, R. E., Hewett-Emmett, D. *Ann. New York Acad. Sci.* 429: 1–640
72. Torriani, A. 1960. *Biochim. Biophys. Acta* 38: 460–69
73. Tu, C., Paranawithana, S. R., Jewell, D. A., Tanhauser, S. M., LoGrasso, P. V., et al. 1990. *Biochemistry* 29: 6400–5
74. Volbeda, A., Lahm, A., Sakiyama, F., Suck, D. 1991. *EMBO J.* 10: 1607–18
75. Von Euler, H. 1912. *Z. Physiol. Chem.* 79: 375
76. Von Euler, H., Funke, Y. 1912. *Z. Physiol. Chem.* 77: 488
77. Weiss, P. M., Cleland, W. W. 1989. *J. Am. Chem. Soc.* 111: 1928–29
78. Westheimer, F. H. 1968. *Acc. Chem. Res.* 1: 70–78
79. Wilson, I. B., Dayan, J., Cyr, K. 1964. *J. Biol. Chem.* 239: 4182–85
80. Wyckoff, H. W., Handschumacher, M. D., Murthy, H. M. K., Sowadski, J. M. 1983. *Adv. Enzymol. Relat. Areas Mol. Biol.* 55: 453–80
81. Xu, X., Kantrowitz, E. R. 1991. *Biochemistry* 30: 7789–96
82. Zeppezauer, M. 1986. See Ref. 7a, pp. 417–34

Annual Review of Biophysics and Biomolecular Structure
Volume 21, 1992

CONTENTS

vi (*continued*)